Appendix C

Draft Geomorphic and Hydraulic Report

Natural Systems Design
Stream & Riparian
Resource Management
P.O. Box 15609
Seattle, WA 98115

September 23, 2015

David Evans and Associates, Inc.
2100 SW River Parkway
Portland, OR 97201

Attention: Mara Krinke

Subject: Geomorphic and Hydraulic Assessment of the Sandy River for the Lolo Pass Road Access Alternatives Study

PROJECT BACKGROUND

Natural Systems Design, Inc. (NSD) is pleased to present to David Evans & Associates, HFWA's Western Federal Lands Highway Department, and Clackamas County Department of Roads and Bridges, this Geomorphic Characterization for the Upper Sandy River regarding the possible relocation of a section of the Lolo Pass Road and bridge. Our services for this project were completed in general accordance with the scope of work and contract dated January 8, 2015.

The Sandy River watershed in northwest Oregon extends from the west flank of Mount Hood to the Columbia River at Troutdale, Oregon (Figure 1). In the last 100 years the Upper Sandy has experienced several major floods that caused substantial flooding, bank erosion and damages to infrastructure. However, from 1964 to 2014 alone the river has experienced 8 of the 10 highest peak flows in its 100 year record of flows. The flood of record occurred in 1964: 61,400 cubic feet per second, cfs) and completely destroyed the bridge and several sections of the road (Portland District Post-flood Report July 1966). In addition to the 1964 event, very large and damaging flood flows also occurred in 1996 (48,100 cfs), and in 2011 (39,000 cfs) where portions of the road upstream of the bridge where severely damaged.

Based on the complete record of flows (100 years), the 1964 storm had a 0.4% probability of occurring in any given year, equivalent to a 250 year recurrence interval flood event. In contrast, the 2011 flood was smaller in magnitude, about a 33 year recurrence interval flood event, but still caused significant erosional impacts along the Upper Sandy shoreline, as well as to public and private infrastructure. During this event several houses were destroyed due to the erosion of bank soils underlying house foundations and a half mile section of Lolo Pass Road, which serves hundreds of residents, was washed out. Over the course of the last several decades the damages have required substantial repairs or total replacement, and tendency for damage to occur with high stage flows has warranted frequent maintenance, which causes the temporary loss of direct access to upstream residential properties and is costly.

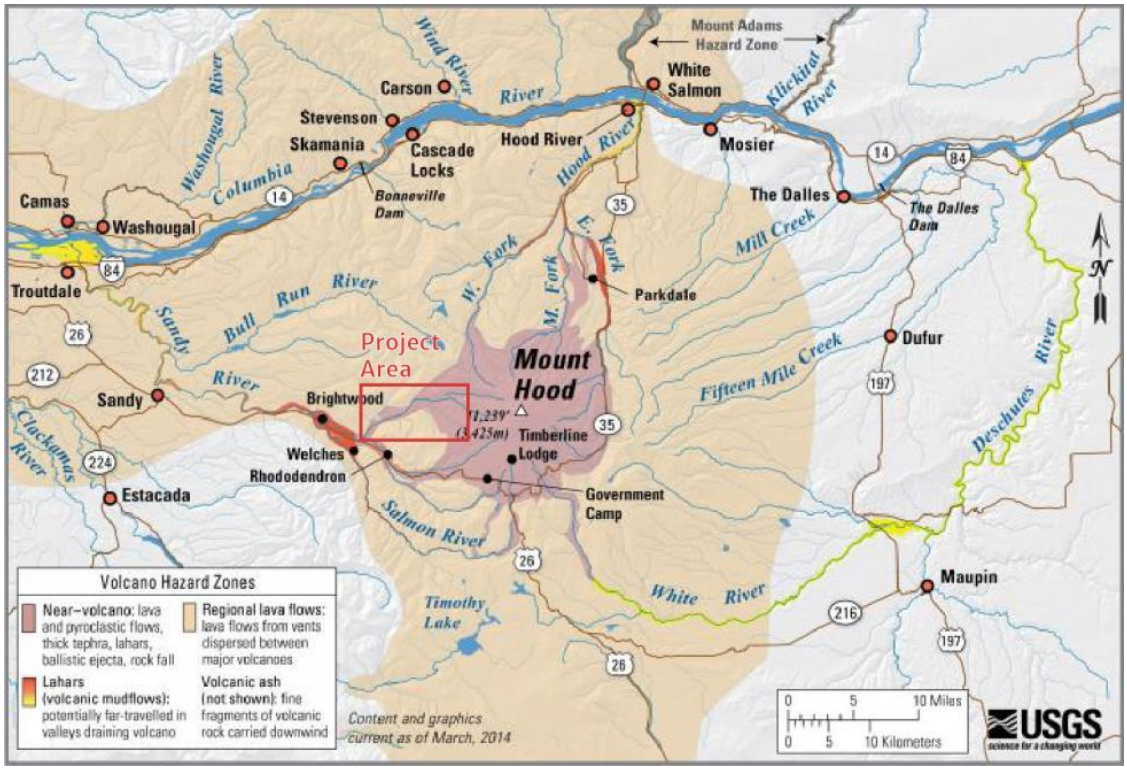

Figure 1. Vicinity Map (USGS Volcanic Hazards Program, 2013).

Clackamas County is committed to improving the reliable access to Lolo Pass Road and bridge upstream of the Zigzag River Confluence, and has teamed with the Federal Highway Administration in an effort to rebuild the bridge in place, rebuild it in a safer location, and move the road as needed.

The primary objective of this geomorphic characterization effort is to evaluate expected long and short term river dynamics, including channel migration and avulsion at the existing and at proposed bridge locations, to determine conditions that could affect new bridge. Another objective is to provide recommendations regarding the elevation of selected storm flows at the existing and proposed locations, with and without the bridge.

PROJECT AREA SETTING

The Lolo Pass Sandy River Bridge is located at RM 43.7, just upstream of the Zigzag River Confluence. The road extends upstream from the bridge another 9.5 miles and provideds access to private residences, a major power line corridor and forest lands. One of the Sandy's largest tributaries, the Zigzag River joins the main stem river from the south at RM 43. A small tributary, Clear Creek, enters the main stem from the north at RM 43.65, immediately downstream of the bridge. Access roads that could be affected by relocating the bridge and road include Autumn Lane, located on the south side of the river, and all residential side streets

serving the Zigzag Village community. The project area extends upstream from the confluence of Clear Creek (RM 43.65) and Upper Sandy River (Figure 2).

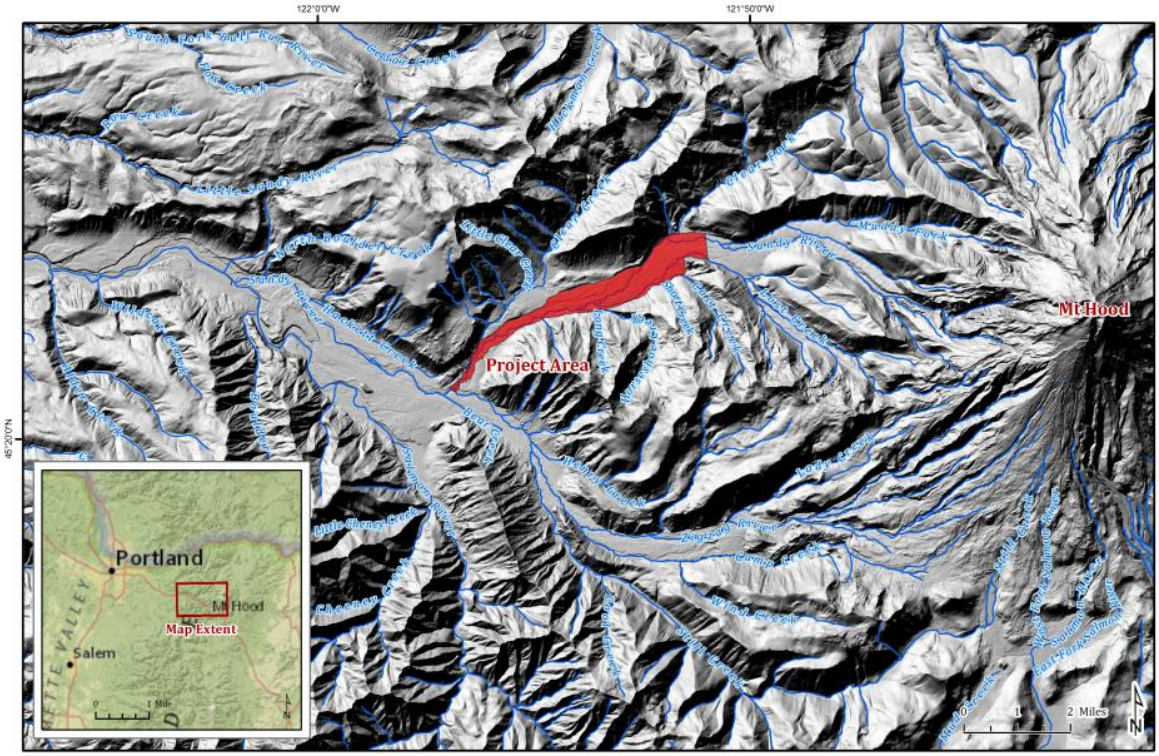

Figure 2. Project Area Map - Upper Sandy River project reach extends from the Salmon River confluence at RM 38 to about RM 49. Data sources: USGS 10m DEM, USGS NHD.

PROJECT CONSIDERATIONS

The project area is located about 10 miles downstream from the river's headwaters on Mount Hood, an active volcano peak 11,239 ft. above sea level. The steep gradient, proximity to the large quantities of sediment eroding from the mountain's flanks, and heavy precipitation all make the Upper Sandy valley especially susceptible to flooding and erosion. The Upper Sandy also lies within the high risk zone of catastrophic mudflows associated with Mt Hood eruptive periods (e.g., Cameron and Pringle 1986; Scott et al. 1997; Pierson et al. 2011).

Two possible bridge sites are currently under consideration; the existing location of the bridge (RM 43.7) and an alternative site located at RM 44.65. The existing bridge stands is a replacement structure for the former bridge, which was totally wiped out during the December 1964 storm event. The proposed alternative site was selected by Clackamas County WFLHD and its consulting staff based on field observations and review of historic aerial photographs dating back to 1952, which suggested the river at that site is less prone to flooding and erosion. However, a study regarding river dynamics, recently completed for Clackamas County by Natural Systems Design, indicate this site may in fact be subject to future migration and avulsion, and a more detailed evaluation of the proposed and existing bridge sites was requested.

The key considerations being addressed with this project include the following:

1. Identify geomorphic processes operating at both bridge sites.
2. Assess the potential for existing and future channel migration and avulsion to negatively affect the bridge at both sites.
3. Evaluate flood surface elevations associated with the 100 year storm event at both sites under both existing and possible future conditions.

GEOMORPHIC SETTING

CURRENT CONDITION

When viewed in plan form, the Upper Sandy River channel follows a southwesterly trend from its sources area to the Zigzag River confluence. The project area is situated in the lower portion of the upper Sandy River Valley and is therefore subject to a relatively steep average gradient, as seen in the Valley Profile (Figure 3). Note that the Lolo Pass Road/bridge project area is situated in a zone ranging from about 0.015 to greater than 0.020.

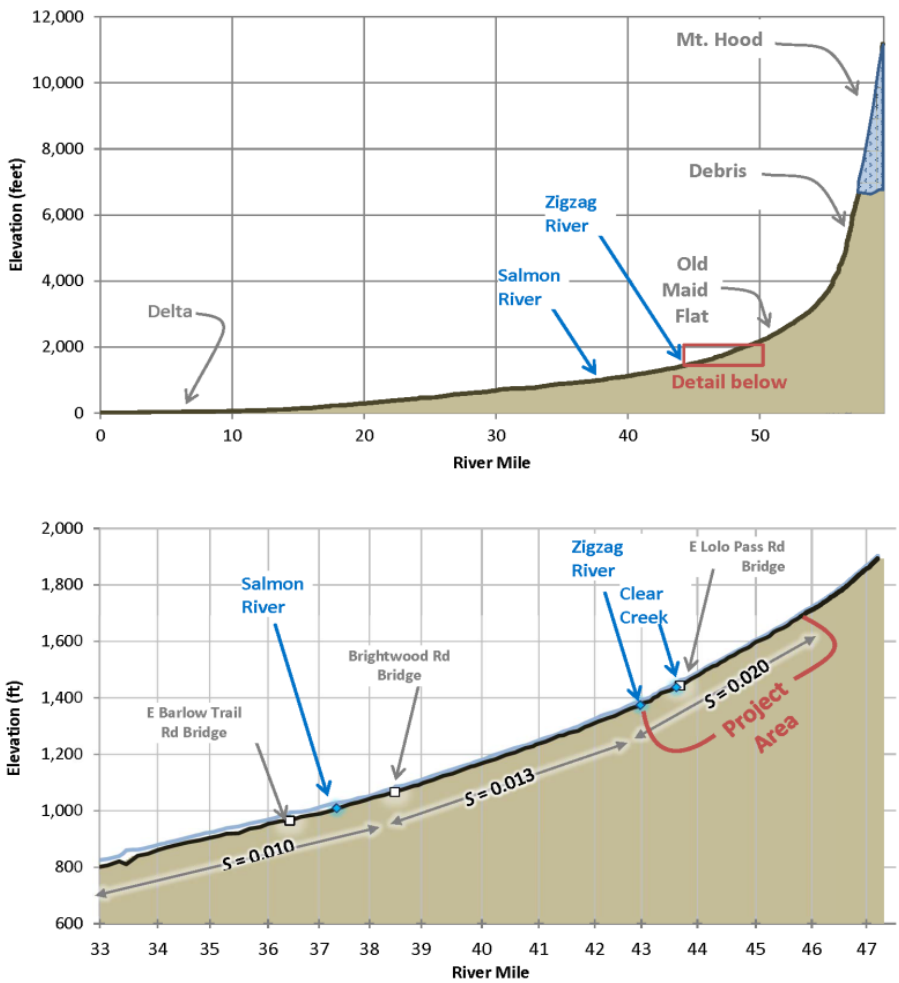

Figure 3. Valley Profile - The project area is situated roughly 10 miles from the Sandy River source area on Mt Hood. Average valley gradients through the project area range from 2 percent above the Zigzag River to 1 percent.

The upper valley floor is very broad and bounded at the edges by steep to moderately graded valley walls. Throughout the upper valley, the active river channel is a braided system consisting of 2 or 3 shallow channels separated by unvegetated to vegetated gravel bars. The braided channel form extends from sediment source areas on the mountain to about RM 44.2, where it transitions to a single stem channel with meander bends that extend to and beyond the downstream end of the project. Topographic features described are most easily observed on the Relative Elevation Maps (Figure 4).

The geomorphic landscape features defining the gross topography of the valley bottom are products of recent watershed- and reach-scale processes; however, they also reflect the history and evolution of the valley. In the case of the area within and upstream of the project area, the history of geologic and geomorphic events has had great influence on present day channel behavior.

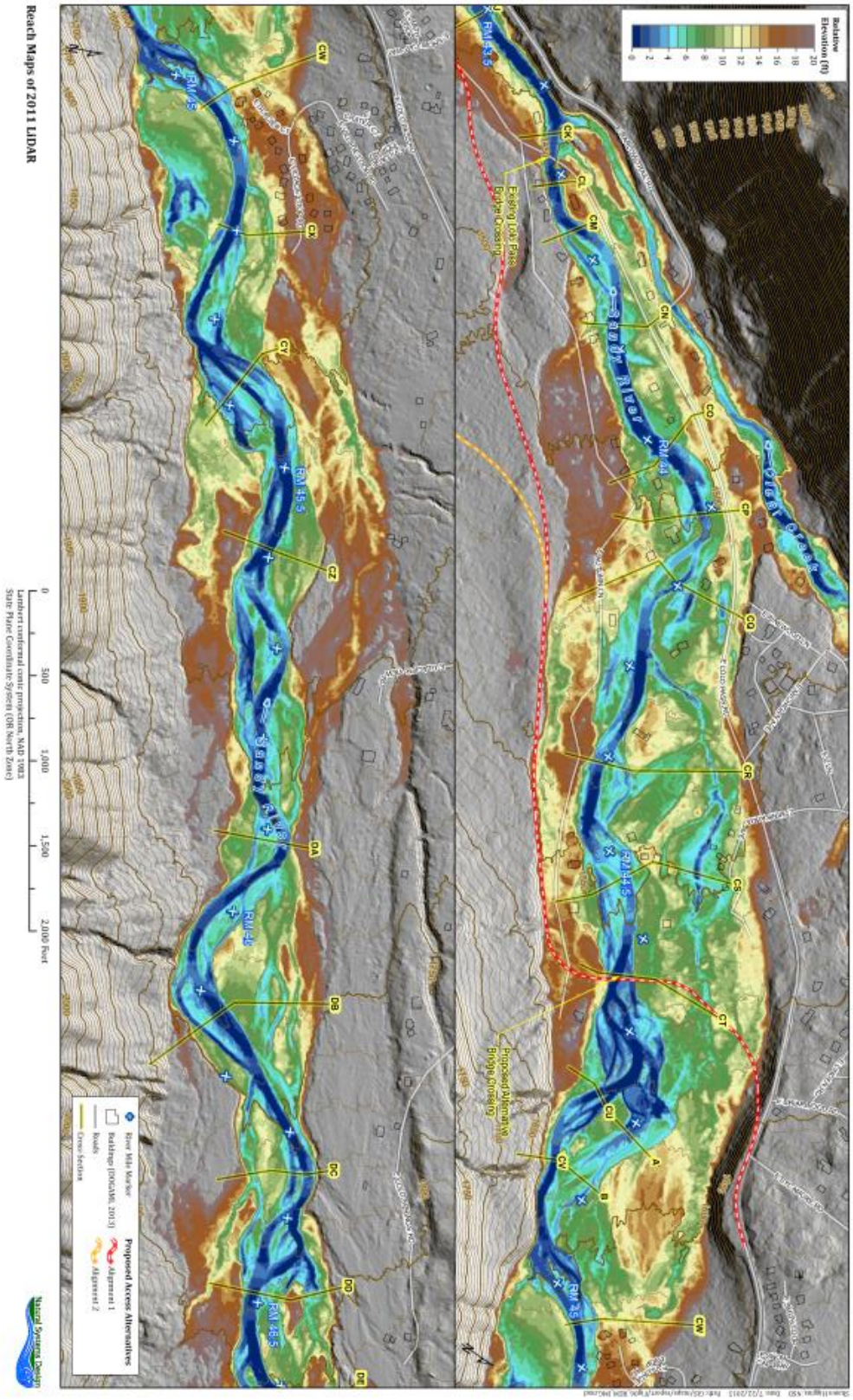

Figure 4. Relative Elevation Map (REM) – This map shows the elevation of land forms relative to the elevation of the river at the time the LiDAR data was collected.

GEOLOGIC HISTORY AND VALLEY EVOLUTION

The Sandy River watershed is underlain by a geologic sequence of Mt. Hood Volcanic rocks and lahar/mudflow deposits, and recently derived sedimentary deposits consisting of alluvial fan and streambed materials. The distribution of these materials is provided in Figure 5 (Sherrod, D.R. and W.E. Scott. 1995).

The Sandy River watershed was carved from Mt. Hood volcanic bedrock by alpine glaciers that have come and gone over the last 60,000 years. Mt. Hood volcanic rocks primarily consist of Andesitic lava flows roughly (65 to 2 million years old). These rocks are generally very hard and impermeable. Lava flows consist of molten rock that flow down the mountain until it cools to form hard volcanic rock. These rocks are exposed at the ground surface along the base of north and south valley walls, and possibly along the north bank of the Sandy River channel a short distance upstream of the Zigzag River confluence. Although most of the major mountain building lava flows ceased roughly 7,600 years ago, the mountain has been active, producing numerous small eruptions of lava, pyroclastic flows and lahars (Scott et al. 1997). Lahars are viscous mudflows composed of volcanic ash, cinders, and silt- to sand-sized rock fragments mixed with water, that originate near volcanic vents. Compared to lahar deposits, volcanic rocks are very resistant to erosion. Many of the more recent lahar events in the last several thousand years flowed down existing river valleys, partially to completely filling the valley.

Lahars move extremely rapidly down the mountain, catastrophically impacting anything in their path. Sedimentary deposits left behind these events are composed of silt to large boulders and are very permeable and sensitive to erosion. The most recent lahars occurred roughly 1,700 and about 200 years ago. The 1,700-year-old event, called the Timberline Lahar, originated at Crater Rock on the upper southwest slope of Mt. Hood, and flowed down both the Zigzag and Sandy River valleys (Figure 4) all the way to the Columbia River (Cameron and Pringle, 1986; Pierson et al. 2011). The most recent lahar event, the Old Maid Lahar, occurred only 200 years ago; it also originated from Crater Rock but flowed down and inundated only the Sandy River valley. Due to its age, and thus it's longer period of compaction, the Timberline lahar deposit is somewhat more resistant to erosion than the Old Maid lahar deposit.

These two lahar events exerted profound influence on Sandy River valley evolution and channel behavior over the last 1,700 years. The Timberline Lahar event completely buried the upper valley bottom and active channel. Following that event, surface water runoff began flowing over the surface of the lahar deposit, quickly forming a new river channel that began cutting downward through the sediment layer (Pierson et al. 2011) (Figure 6a, b, c) . As the river cut downward, it also widened out as it eroded sidewalls composed of lahar deposits. As the river widened its corridor, it created space for more complex channel patterns by migrating back and forth laterally across the valley and widening the floodplain by further eroding the mostly fine sediment of the lahar deposit. Over time, this process resulted in a landform consisting of one or two broad, flat topped terraces at higher elevation that the incising river channel and floodplain (Figure 6d).

When the Old Maid Lahar event occurred it completely filled and/or blanketed the upper portion of the valley landforms (upstream of the Zigzag River confluence) and partially filled the valley downstream of the Zigzag River confluence, leaving only the Timberline terraces emergent, forcing the river to reform again at the top of the new deposit to begin the whole process over again (Figure 5 e and 5f). Since the occurrence of the Old Maid Lahar event, the upper valley landscape (at and above the project area) has been subject to sediment deposition and is referred to as the Old Maid Flats. This area still functions as a zone of deposition, and is prone to aggradation of the channel and valley bottom, coupled with periodic episodes of channel widening associated with large sedimentation events. The topography of the Old Maid Flats area is most easily viewed on REM Maps shown in Figure 4.

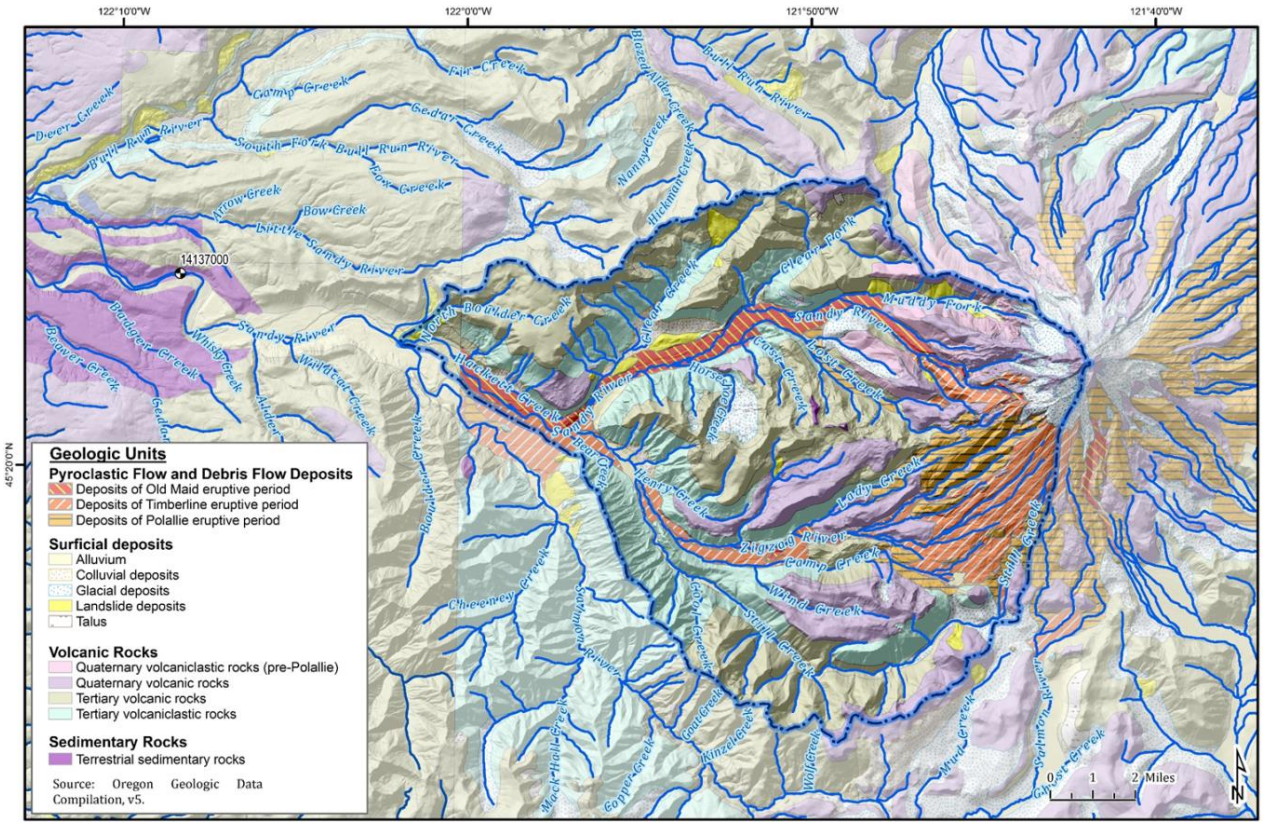

Figure 5. Geology Map. Base map data from: USGS Mt. Hood (1983) and Oregon City (1982) Quadrangles.

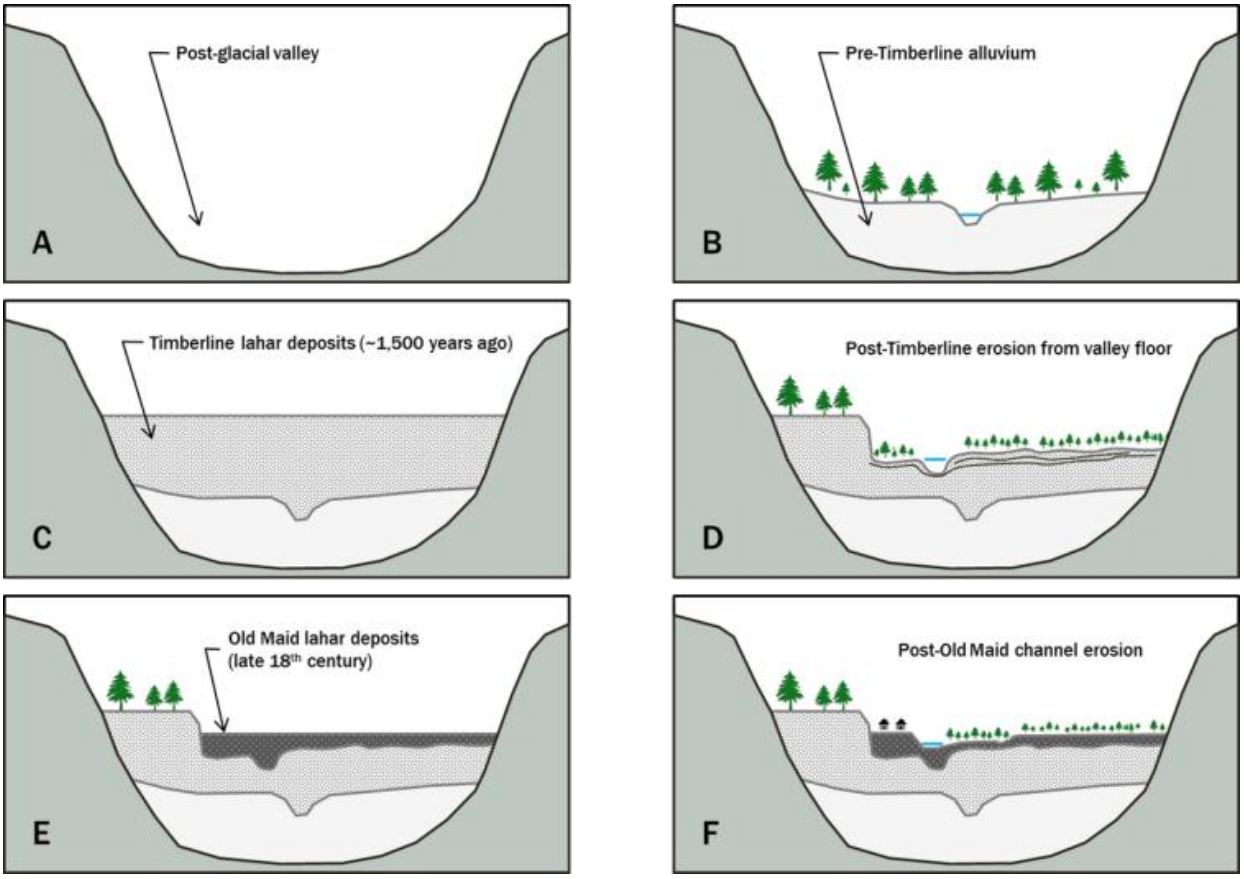

Figure 6. Watershed Scale Valley Responses to Lahars - The effects of Timberline and Old Maid lahars on the Upper Sandy River valley begin with sketch C, which depicts how the mudflow buried the valley floor to depths up to 100 feet. Over the course of next 1,500 years, the river channel cut downward and widened the floodplain, creating terraces composed of Timberline lahar (D). The Old Maid lahar buried the active channel and floodplain, but not the high Timberline terraces about 200 years ago, forcing the process of incision and channel/floodplain widening to start over again.

EVOLUTION OF THE UPPER SANDY RIVER CHANNEL

If no other major depositional events were to occur in the valley, the river would continue down cutting to a stable elevation somewhere close to the pre-Timberline elevation, where further incision would likely cease. However, in the 200 years since the Old Maid Lahar event, several small lahars and numerous debris flows consisting of eroded volcanic and lahar sediments have coursed down the mountain slopes and through the Zigzag and Sandy River valleys. With each event, the elevation of the river bed increases by some amount, changing local and sometimes reach-scale channel gradients, forcing the river to constantly adjustment.

The changes in channel form recorded in the Old Maid Flats portion of the river are the result of numerous, periodic episodes of smaller scale geological processes capable of bringing large volumes of sediment in from upstream sources. These processes include landslides, debris flows, and debris torrents, the products of which consist of reworked sediments from stockpiled lahar deposits on valley walls high in the watershed. Sediments produced from these processes are typically transported downstream either by the momentum of the originating event or

during high stage flows and deposited on the Old Maid Flat area as thick to thin blankets of sediment forming an alluvial plain. From there, sediment can be mobilized and transported further downstream by storm flows with sufficient transport capacity, which of course can vary widely depending on the magnitude of the storm event. The process of remobilizing and transporting this material has resulted in the formation of gravel/cobble bars and relatively shallow braided channels separated by the bars.

The project area (Figure 2), located within the downstream portion of the Old Maid Flats area, is subject to frequent and sometimes profound changes in channel form and pattern. The changes are typically driven by the deposition of large sediment volumes, and the arrival of large woody debris. The most frequent changes to channel form include channel widening and migration, both of which occur in response to sediment deposition within the existing channel.

The adjustment can be seen from historical documents covering the last 100 years. Based on a 1914 Sandy River survey, the river had a single to multi-channeled planform (Figure 7). The survey was completed roughly 100 years after the occurrence of the Old Maid Lahar, and the depicted channel probably represents the transition of the river from braided to single stem as it worked through the catastrophic infilling of the valley with lahar sediments. The 1952 aerial photograph shows a portion of the project area, and a largely single stem channel with several relatively small radius bends. The 1952 photograph also shows that the land adjacent to the channel is heavily forested, and that the channel has cut down (incised) into underlying sediment.

A comparison of the 1952 and 1961 aerial photographs indicates that the channel pattern changed little over that 9 year time period. However, the 1961 photograph shows that the channel widened somewhat from sediment deposition, and that vegetated bars had begun to develop (Figure 8), suggesting a large volume of sediment entered and deposited within this channel section sometime just prior to the date the photo was taken.

The channel pattern throughout the project area changed dramatically in 1964 in response to the major storm during which an enormous volume of sediment was transported and deposited. The 1964 storm was (and is still today) the largest storm flow on record, estimated to have been equivalent to a 250 year storm event, with a peak flow of 63,000 cfs. Pre- and post-1964 event changes are shown in Figure 8).

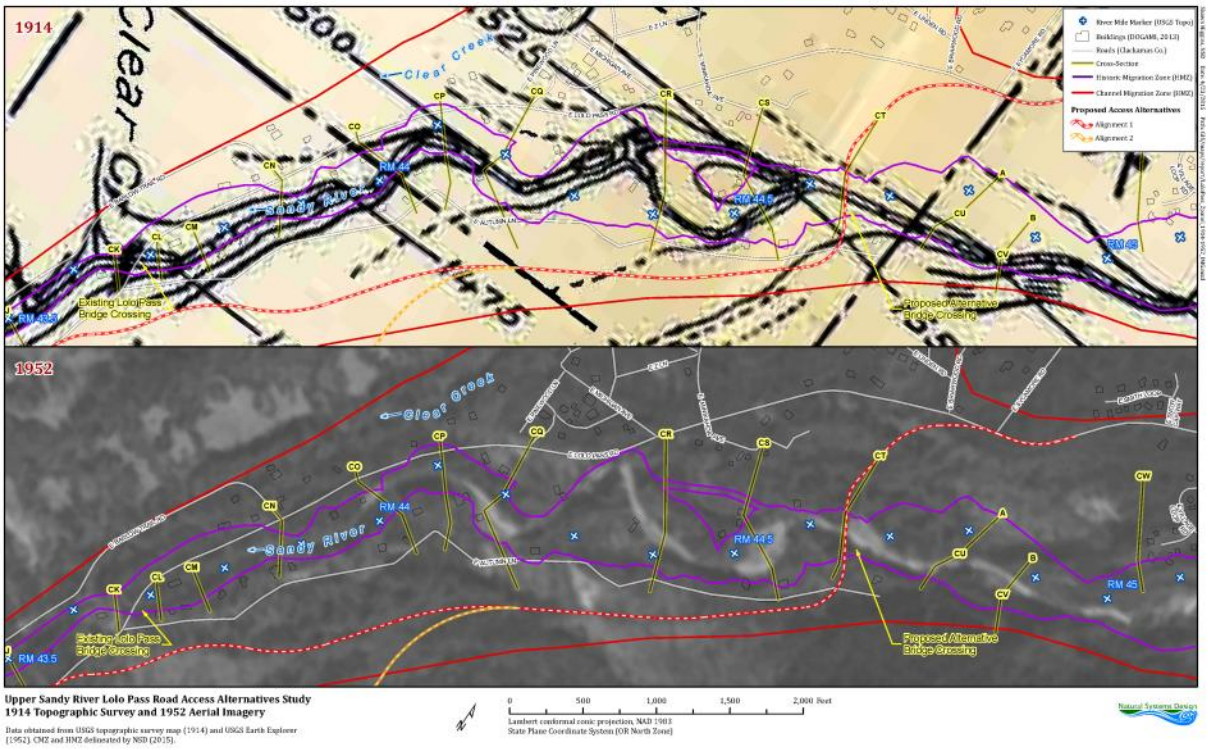

Figure 7. Comparison of the 1914 survey map and the 1952 aerial photograph shown with the existing and proposed bridge sites and road alignments. This comparison shows a transition of the river from at least two channels (1914) to a single stem channel with well developed bends (1952).

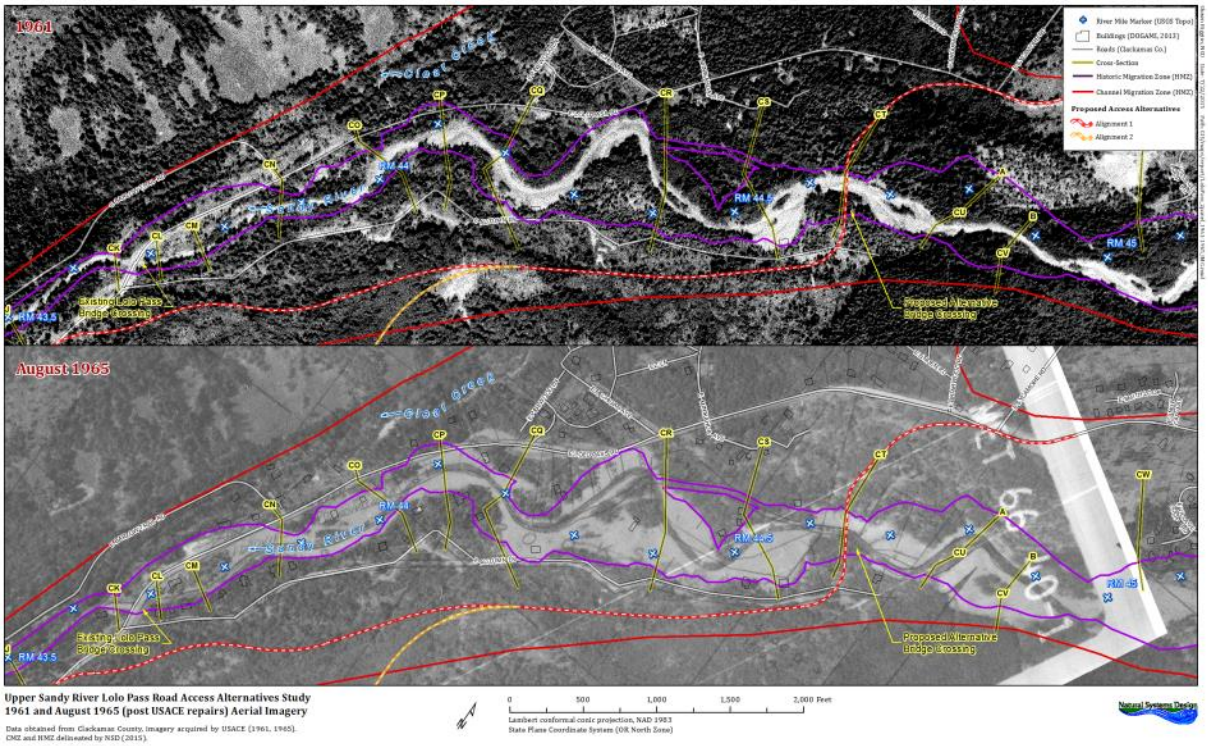

Figure 8 (previous page) . Comparison of 1961 and 1965 aerial photographs. Note that the 1961 photograph presents the river prior to the December 1964 storm event. The 1961 channel is wider the 1952 channel with considerably more sediment in the visible active channel corridor indicating a substantial sedimentation event. The August 1965 photograph presents the river after the 1964 storm and shows the effect of the very large volumes of sediment deposited during that event. Note the extent of channel widening and bend growth (channel migration). The 1964 storm blew out the Lolo pass bridge, and three road sections located at RM 48.9, and from RM 44.1 to 44.4.

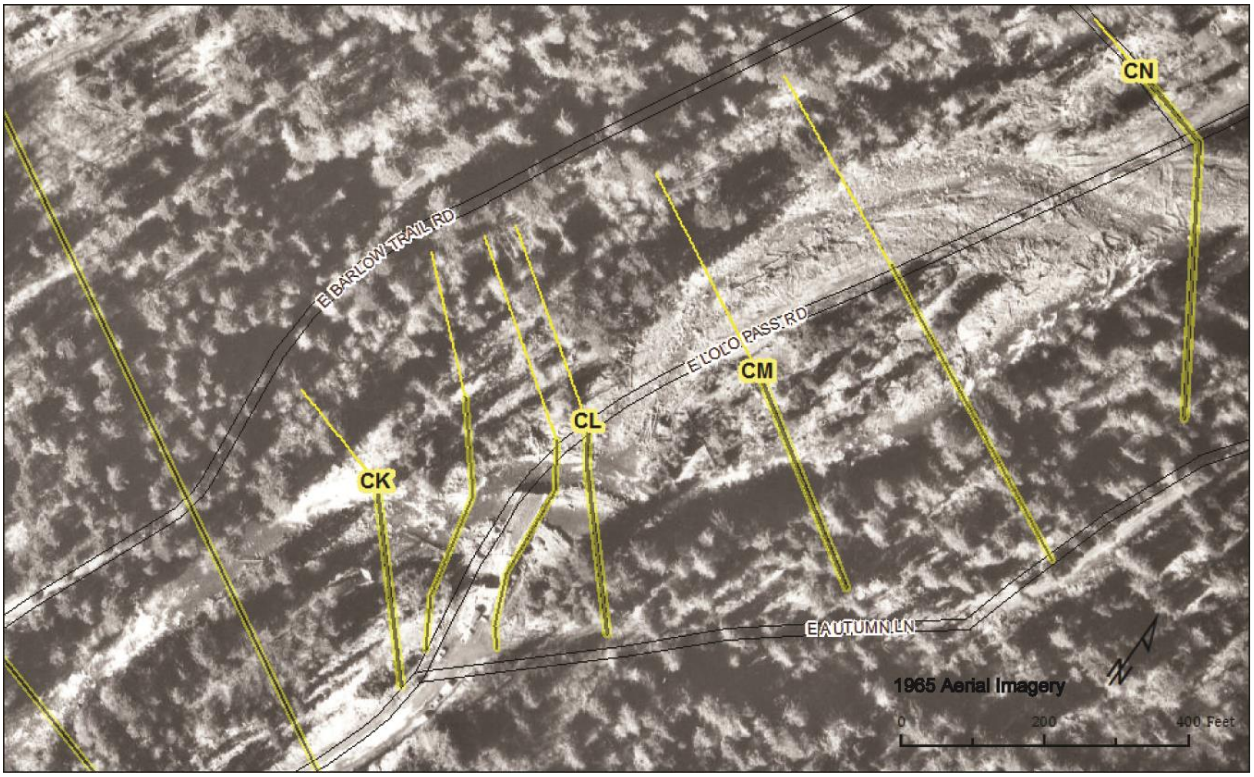

Figure 9. Enlargement of aerial photograph taken in February 1965. Note the width of the 1964 channel (150 to 200 feet) which increased during the storm to accommodate the storm flow. Also note the new channel formed during the event that tore out E Lolo Pass Road. The avulsion extended from cross section CL to cross section CN.

Close inspection of the 1965 photograph yields several observations crucial to this characterization. First, the active channel widened almost everywhere by a factor of 2 or 3 over the channel width shown in the 1961 aerial, eroding alluvial river banks and increasing the channel corridor width from a minimum of 150 to 200 feet up to 1,000 or 1,200 feet. Erosion and channel widening was a primary factor leading to the loss of Lolo Pass Bridge; Figure 9 presents an enlargement of an aerial photograph taken in February 1965, prior to any repairs.

Second, channel widening was accompanied by an increase in bend heights resulting from channel migration, new bends developed, channel sinuosity increased, and new channels cut through forested areas abandoning the previously occupied channel (a process called avulsion). Bank erosion associated with bend migration was the leading cause of severe damages along Lolo Pass Road and Autumn Lane. Third, aggradation of the channel during the storm event was a catalyst for channel avulsions between RM 44.3 and 44.5, and throughout the upper valley.

Since 1964, the channel has continued to change. Aerial imagery dated February 1965 shows the channel down cut into the 1964 sediment deposits. Portions of the channel appear to have been mechanically altered, presumably by the Army Corps of Engineers. Throughout, and upstream of, the project area the river channel was re-graded and put back into its pre-1964 alignment by the Army Corps of Engineers. These actions served to shorten the amplitudes of some bends by 100 to 200 feet. In addition to altering the channel pattern, all woody debris was removed from the active channel.

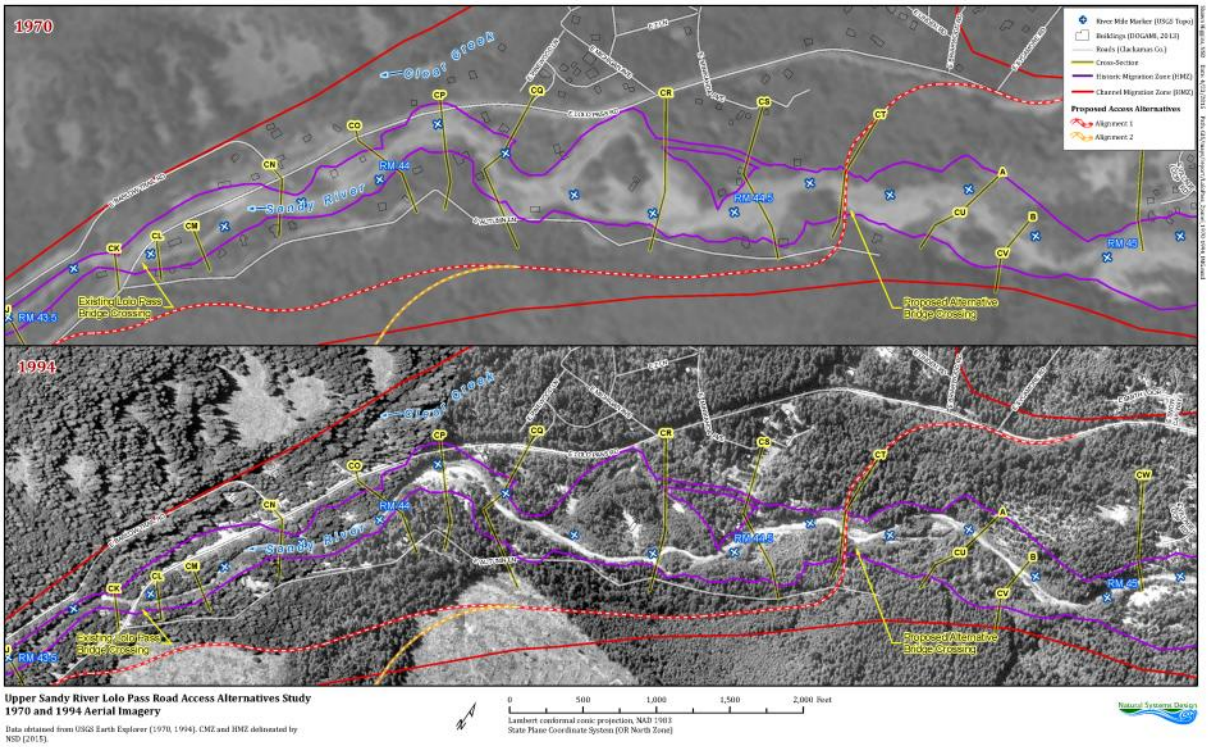

Figure 10. Comparison of 1970 and 1994 aerial photographs. The 1970 channel form is largely unchanged from 1965. Note that by 1994 the channel width had decreased indicating that the channel had incised into 1964 sediment deposit.

From 1970 to 1994 (Figure 10) most of the changes observable from the aerial photographs include minor bank erosion due to channel migration, and a substantial channel avulsion at RM 44.25 where the channel moved away from Lolo Pass Rd and took up residence along the left bank (Figure 11). The new channel was created during the 1964 storm event, but was closed by the Army Corp when they regraded the channel and pushed the river back into the 1961 alignment.

From 1994 to 2008 (figures 10 and 12) both channel widening and bend migration increased substantially. The bends re-graded by the Corps upstream of the Lolo Pass Bridge increased in amplitude and migrated southeast back into the 1964 channel. Much of the widening can be attributed to the 1996 storm event, which is estimated to have been close to the 100 year recurrence interval storm. The apex of a large bend at RM 44.1 (cross section CP) migrated very close to E Lolo Pass Road. This same bend caused substantial road damage in 1964.

The channel continued to evolve from 2008 to 2012 (Figure 12) with the most significant areas of change occurring in response to the 2011 storm event. This storm caused substantial erosional damage along channel banks and, in some areas, threatened the total loss of several residential structures. It is worth noting that the evolution of the channel followed in suit with the changes observed after the 1964 and 1996 storms.

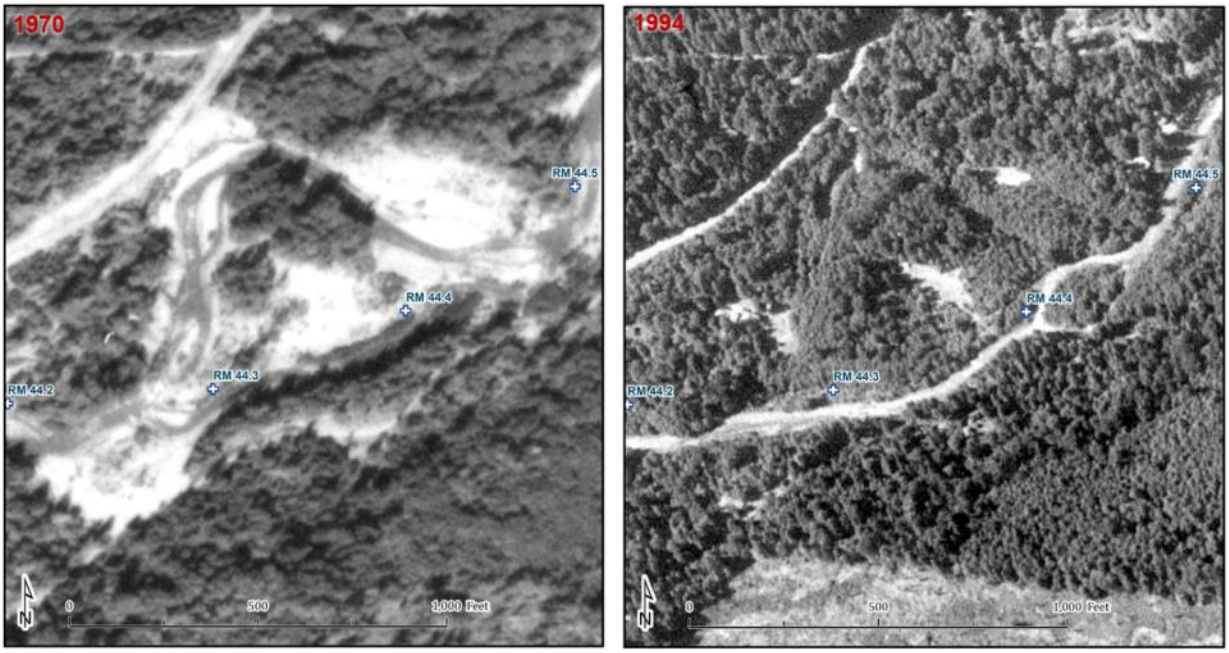

Figure 11. Enlargement of both 1970 and 1994 aerial photographs showing an avulsion of the main stem channel. Data sources: University of Oregon Libraries.

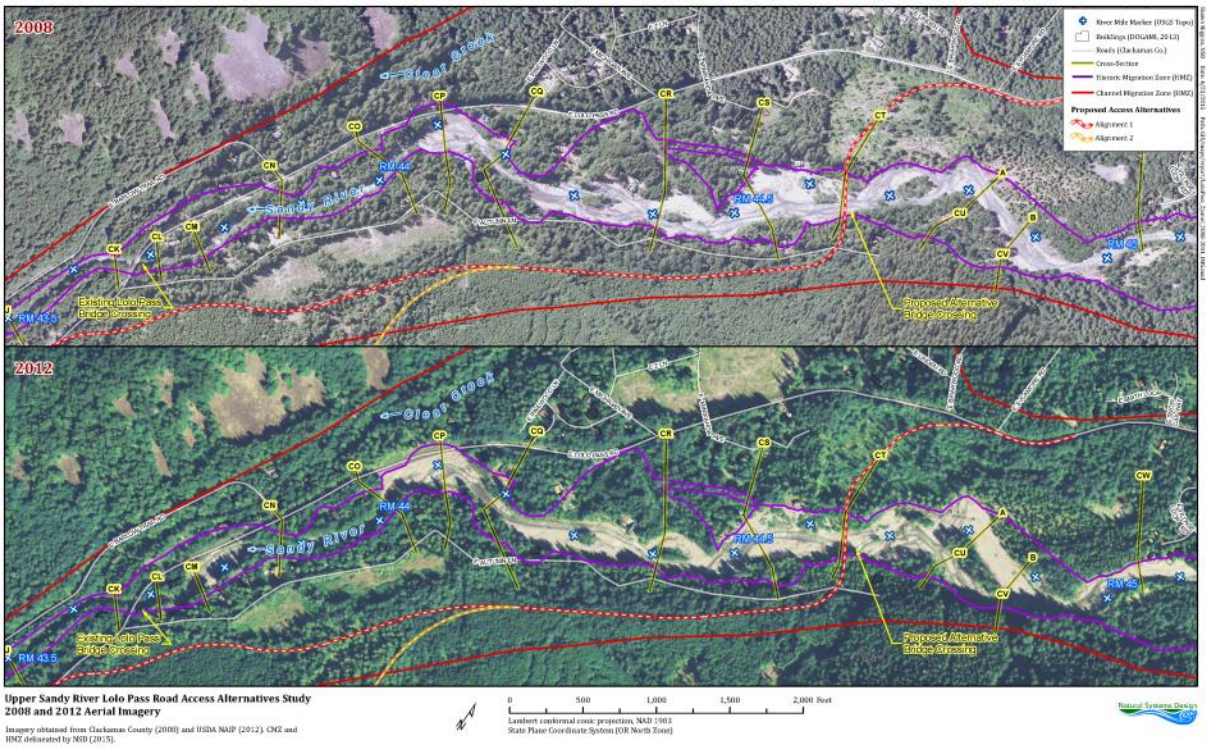

Figure 12. Comparison of 2008 and 2012 aerial photographs. Note the proximity of the large bend at RR 44.1 (cross section CP) to E Lolo Pass Road in 2008 and its location in 2012. This bend caused substantial road damage during the 2011 storm event. Note also the channel avulsion between RM 44.7 and RM 44.9. The avulsion likely took place during the 2011 storm event.

Comparison of the active channel captured in each dated aerial photograph indicates that the major bends discussed above are moving downstream, parallel to the valley centerline. Three traces showing the form of the channel in 1952, and two others showing the channel form following the 1964 (August 1965 photo) and 2011 (2012 photo) show that the overall trend of bend migration is in the downstream direction (Figure 13). Also note that the bend experiencing the most pronounced (rapid) downstream migration is located immediately upstream of the proposed bridge site.

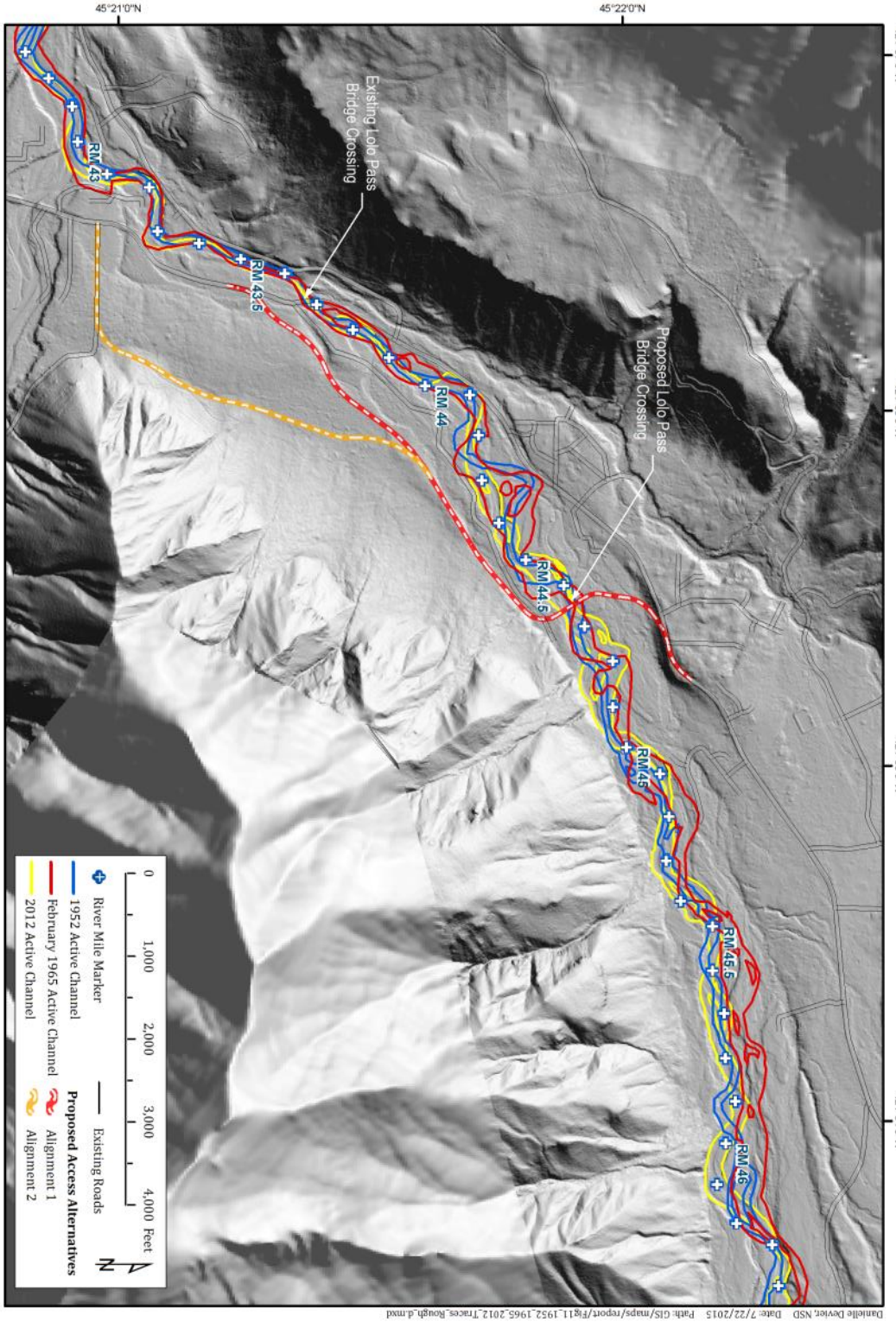

Figure 13. Comparison of 1952, 1965 and 2012 active channel traces digitized from time series aerial photographs.

CHANNEL FORM AND PROCESSES

The preceding section described the evolution of the channel as it responded to the Old Maid Lahar and the three biggest storm events of the last 50 years.

Channel widening has occurred primarily in response to the formation of vegetated bars (islands) stable enough to split flow and stand up to the force of the river at the 33 year recurrence interval flood event of 2011. Upstream of the Zigzag River vegetated islands appear to be developing within the braided portion of the river. This channel type, called anabranching, consists of two or more channels separated by vegetated islands. In well-established anabranching rivers the islands can persist for decades or centuries and are at approximately the same elevation as the surrounding floodplain (Bridge 1993). The relatively rapid evolution of the river from the single thread channel of the USACE to one comprised of anabranching and braided areas can be explained in part the river's gradient, discharge and the median grain size of the bed material, all of which play important roles in channel form (straight, anabranching, braided). The variation in channel with channel gradient and grain size /discharge is shown in Figure 14.

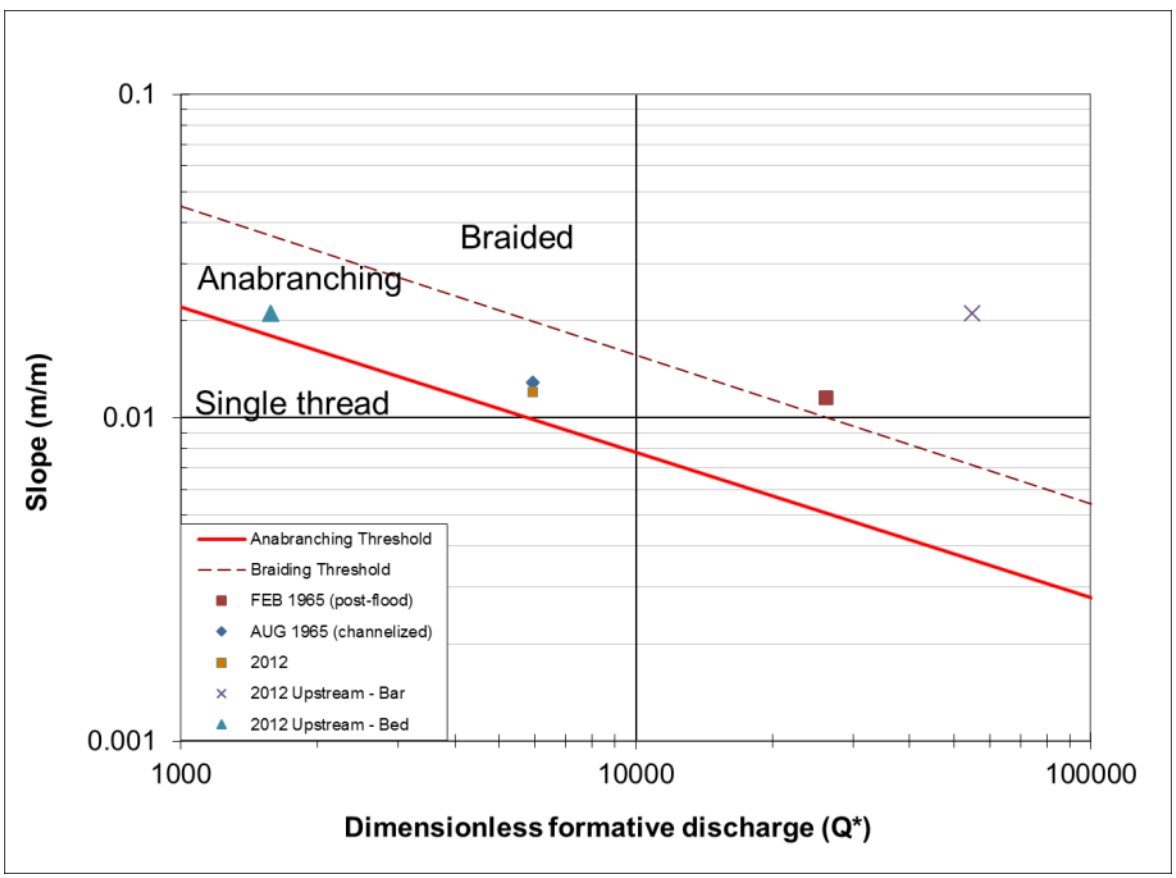

Figure 14. Anabranching Threshold for Sandy River. After Eaton et al. 2010.

Following the method of Eaton et al (2010), aggraded segments of the upper project area plot as a braided channel (2012 Upstream-Bar, Figure 14). Plotting up the same segment using the D50 of the 2012 incised channel, the river plots in the anabranching domain (Figure 14). Immediately following the December 1964 flood the Sandy below the Zigzag River confluence plots up in the braided channel domain due to the assumption it had a smaller D50 (Figure 14). The channelized 1965 and 2012 channel both plot well within the anabranching domain, indicating that the river is unstable as a single thread channel (Figure 15). This analysis shows that the river will be most stable in a braided and/or anabranching channel pattern, which requires a substantially wide corridor to allow the development of 2 or more channels.

As discussed earlier in this report, the upper river banks are composed of mud flow deposits and sediment derived from the mud flows, all of which are highly sensitive to erosion. The river has been able to substantially erode its banks during large flood events, causing recession of the banks from as little as a foot or two, to more than 100 feet at a time. The processes typically associated with the bank erosion include, at a minimum, channel widening associated with channel aggradation, and channel migration, which is defined as the physical movement of the river channel.

The migration of braided channels is often coupled with the development of bars within the active channel, and is more typically associated with higher channel gradient, and a supply of sediment that exceeds the transport capacity of the flow. Braided channel systems consist of multiple, relatively shallow channels separated by un-vegetated, relatively loose gravel/cobble bars. At bank full flows, the braids coalesce into a wide shallow channel. Both the bars and channel alignments are unstable and subject to frequent mobilization and reorganization during any flow capable of entraining bar and bed materials. When large volumes of bedload are transported into a river segment lacking the capacity (channel gradient, flow energy) to move the material the channel aggrades and widens. Channel braiding is indicative of a bedload supply that exceeds the river's transport capacity. These conditions can also promote aggressive channel migration, as seen in Figure 13.

Channel avulsion is a form of migration where the river abandons its current channel to occupy a newly formed, or older abandoned channel. The avulsion can take place abruptly, during a single storm event or gradually over a period of several storm events. Avulsions occur when the current channel fills with sediment, or when flow is diverted out of the main channel by some combination of sediment and large woody debris whose volume is sufficient to obstruct flow. A key point here is that channel migration and avulsion are both driven, in large part, by river discharges strong enough to move sediment and erode banks; the presence of erodible bank soils; and deposition of sediment and large tree snags on the channel floor and bar surfaces.

CHANNEL MIGRATION AND AVULSION HAZARDS

The project goals established for this focus on assessing historic and current river conditions and erosion trends as an approach for identifying a suitable crossing site for the Lolo Pass Bridge.

Maps projecting the future channel migration zone (CMZ) offer an effective vehicle for identifying channel areas subject to substantial bank erosion and recession caused by channel widening and channel migration. The CMZ defines the probable extent of migration over the course of a specified period of time. The width of the estimated CMZ is based on historic rates of migration. The CMZ should be sufficiently wide to accommodate future migration trends and channel widening.

A Sandy River CMZ map, originally prepared by the Department of Emergency Management was used to help evaluate both the existing and proposed bridge locations with respect to future migration and avulsion risks. This original map, dated 2011, was modified to incorporate aerial photographs and LiDAR (2013), made available since the publication of the DOGAMIs maps. The modified CMZ maps are available for review in the report entitled 'Upper Sandy River Flood Erosion Hazard Mitigation Evaluation' (Natural Systems Design, 2015), available on the Clackamas County Website. Figure 16 shows CMZ map coverage for the Lolo Pass Road bridge project area and upstream river segments.

The modified CMZ map now includes the effects (channel responses) of the 2011 storm event, and shows all active channels as of the 2012 aerial photograph, and all potential avulsion channels (AHZ). The modified CMZ map was also extended from RM 43.8, the upstream terminus of the DOGAMI mapping effort, to RM 47.5.

One of the more striking differences between the original and modified maps is the wider CMZ, which was increased to better account for rapid migration and channel widening that occurred during the 1964 storm event, as well as the 1996 and 2011 storm events. On average, the adjusted CMZ is about 2,000 feet wide throughout the project area. The increase is based on several factors; migration recorded since the 1970 aerial photograph, the tendency of river bends to migrate downstream as well as laterally, and potential for rapid widening of the active river channel with the next significant, 75 to 100 year recurrence interval storm event.

The consistency of the CMZ width throughout the project area, even in places that have shown little or no migration and channel expansion, is intended to account for future variability, as seen in the historic record. At present, the Upper Sandy River valley bottom and channel, including the project area, is very young (only 200 years old), and will therefore be subject to extreme swings in channel processes, ranging from incision to channel widening, as the channel continues to respond to the Old Maid Lahar and to large sediment loading events.

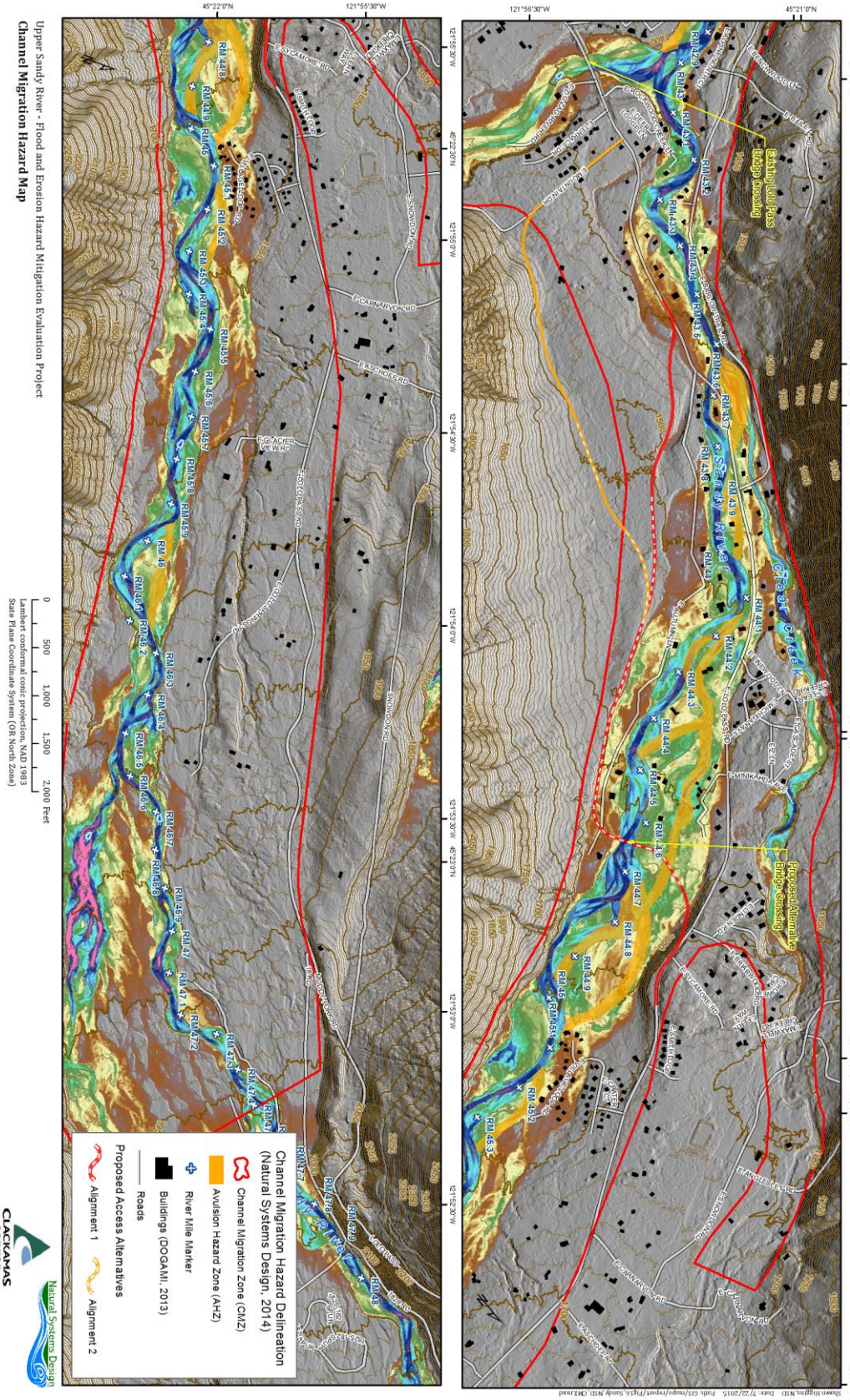

Figure 15. Channel Migration Zone and Avulsion Hazard Area map for the Lolo Pass Bridge Replacement project area and upstream river sections.

The width of the modified CMZ from RM 43.8, the terminus of the DOGAMI effort, to RM 44.7 increases substantially from upstream and downstream channel sections. This section of the CMZ was mapped to accommodate uncertainties regarding the composition of the landform separating the main stem river from Clear Creek. LiDAR or REM maps show no clear visual evidence that the main stem Sandy River channel has crossed over or resided on the landform in the past, although there is evidence that Clear Creek has migrated into the landform. In contrast to these observations, all available geologic and soils maps, and NSD field observations made in in 2014, indicate the landform is underlain by Lahar or alluvial soils, To accommodate these contrasting findings, a conservative approach was taken to defining the CMZ with respect possible future channel movement, and the CMZ was set to include both the Sandy River and Clear Creek. It should be noted that further refinement of the delineated CMZ boundary may be accomplished as additional data become available from a field assessment of the proposed alignments or subsurface investigations that include geotechnical borings.

Particularly important to this project is the newly gained information regarding potential avulsion hazards in the vicinity of both bridge sites. These hazard areas consist of previously abandoned channels with bed elevations low enough to recapture main stem flow during a high stage flow event. Figures 16a and 16b display the avulsion that took place immediately upstream of the proposed crossing during the storm of 2011. Figure 16a shows an abandoned channel located just west of the apex of the active bend (RM 44.8), which likely carried flow during bank full flows and appears capable of capturing main stem flow in an avulsion of the main channel. Note that the avulsion path extends west from the active bend apex along the north alluvial terrace, and crosses the proposed road alignment (cross section CT) adjacent to RM 44.66.

Figure 16a also shows the land surface on the south side of the channel between cross sections CV and CU was roughly 8 to 12 feet higher than the elevation of the water surface, and probably would not have been flagged as an avulsion hazard area in 2008. Figure 16b displays the same river section as shown in 2011 LiDAR imagery, the data that was collected after the 2011 storm event. This image indicates that the avulsion was caused by the aggradation of the 2008 channel by sediment.

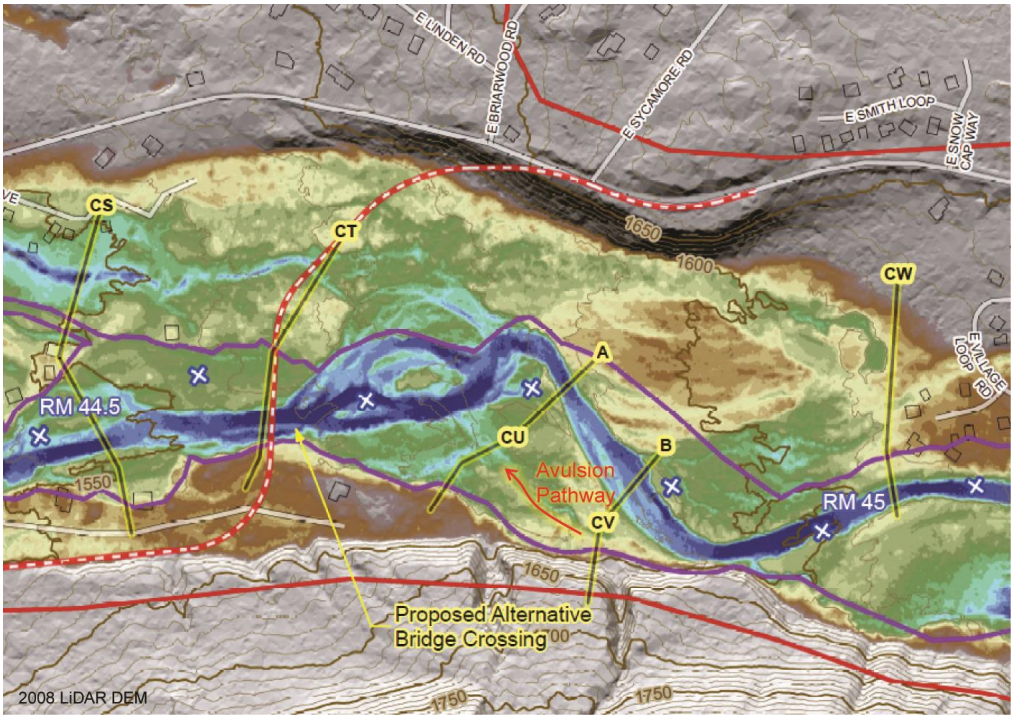

Figure 16a. 2008 LiDAR with REM processing showing the main stem channel in 2008.

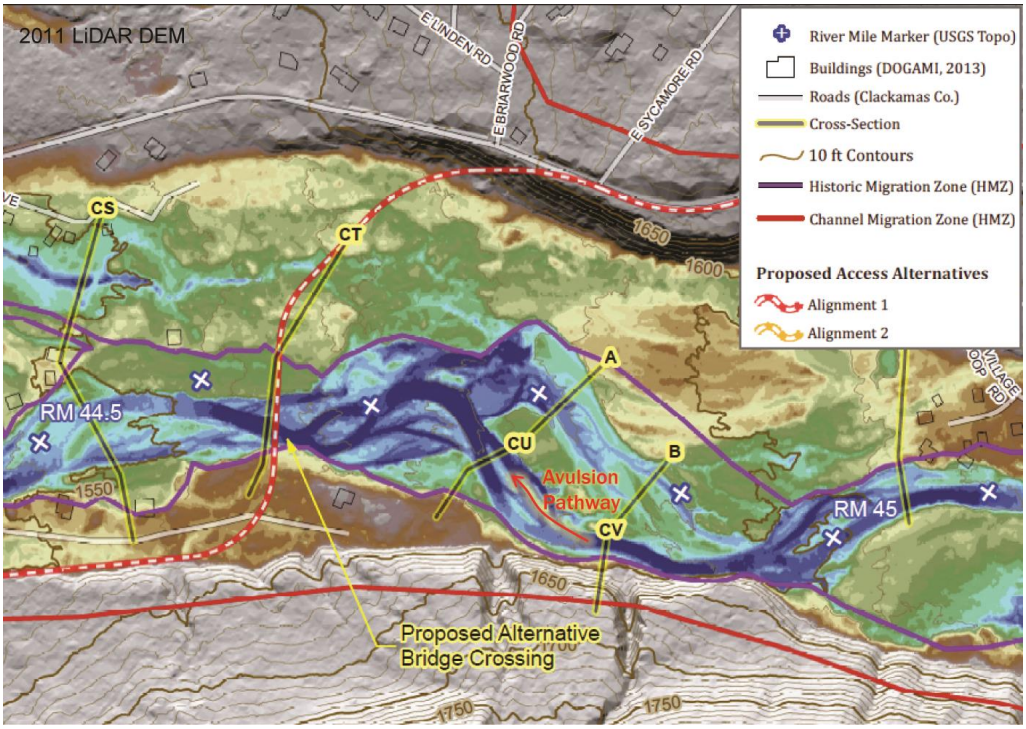

Figure 16b. 2011 LiDAR with REM processing showing the main stem channel in 2011.

FLOOD FREQUENCY ANALYSIS

The Upper Sandy River watershed upstream of Clear Creek encompasses an area of about 42 square miles on the western flank of Mt. Hood. Peak flow events in the project reach predominantly occur in the fall and winter in response to prolonged, heavy rainfall associated with atmospheric river storm events (Table 1). Atmospheric rivers not only deliver large amounts of precipitation, but are generally accompanied by warm air (7-10° F above normal) that increases freezing levels to over 6,000 feet and results in a much larger portion of the watershed area receiving precipitation in the form of rain as opposed to snow. There is a transitional snow zone with shallow snowpack at lower elevations in the watershed (generally between 1,500 and 3,900 feet in elevation) that can melt rapidly during rain-on-snow events and produce additional runoff contributing to floods.

There are no historical streamflow data available to calculate flood frequency statistics for the project reach. USGS has maintained a long-term streamflow gaging station near Marmot that has been active since 1912. The drainage are of the gaging station at Marmot is 264 square miles. Flood frequency statistics for ungagged subbasins can be derived from the USGS gaging station data if the ungagged watershed has an area between 50 and 150 percent of the drainage area at the gaging station. Drainage area of the project reach is only 16% of the drainage area at Marmot.

USGS has developed a set of regression equations to estimate peak discharge for ungagged watersheds in western Oregon (Cooper, 2005). Regressions were developed from historical streamflow data at 107 stations in a flood zone covering the higher elevation watersheds with a mean elevation greater than 3,000 feet. The USGS regressions estimate peak discharge as a function of drainage area, watershed slope, precipitation, and the range of winter temperature. Input watershed characteristics are derived from information derived from USGS Digital Elevation Models and precipitation data from the Oregon Climate Service (Table 2). Resulting estimates of peak discharge at return intervals ranging between 2- and 500-years are summarized below in Table 3. Average prediction errors for the USGS regression equations range between 32 and 39 percent.

A key assumption in the use of historical streamflow data to estimate flood frequency for a given recurrence interval is that of stationarity. That is, that mean and variance of the historical data do not change over time. Streamflow characteristics in mountain drainage basins of the Pacific Northwest; however, are sensitive to changes in temperature that alter the relative amount of precipitation falling as rain as opposed to snow (Elsner et al., 2010). Watersheds that have a large area within the transient snow zone, in which snowpack persists for relatively short durations and can melt rapidly during rain-on-snow events, are particularly sensitive to changes in climate (Hamlet and Lettenmaier, 2007). The frequency of extreme precipitation in Oregon has increased over recent decades (Mass et al., 2011) and investigations of future climate scenarios predict a 15-39% increase in the magnitude of future atmospheric river events and a nearly threefold increase in the frequency of atmospheric rivers by 2100 (Warner et al., 2015). Historical streamflow trends in the Sandy River show a significant increase in winter

streamflow and concurrent decreasing trend in spring runoff at the USGS gaging station at Marmot (Jefferson, 2011). Model simulations of future conditions in the Sandy River basin predict an over 80% reduction in snowpack, 40% increase in January streamflow, and a nearly 20% increase in the 100-year peak discharge by the end of the century (Hamlet et al., 2013; Tohver et al., 2014).

Table 1. Summary of peak flows recorded at the USGS gaging station near Marmot (#14147000).

Rank	Date	Peak Flow at USGS Gage at Marmot (cfs)
1	December 22, 1964	61,400
2	February 07, 1996	48,100
3	January 16, 2011	39,000
4	February 23, 1986	37,800
5	January 20, 1972	36,200
6	December 02, 1977	34,500
7	November 25, 1999	34,400
8	January 02, 2009	30,000
9	January 06, 1923	29,200
10	November 24, 1960	27,500

Table 2. Watershed characteristics used as input to regional regression equations for flood frequency.

Drainage Area (sq. mi.)	42
Mean watershed slope (degrees)	21.4
2 yr, 24 hr Precipitation (in)	3.7
Mean min January temperature (F)	26.0
Mean max January temperature (F)	36.7

Table 3. Estimated peak discharges in the Upper Sandy River above Clear Creek based on USGS regression equations for flood zone 2A (Cooper, 2005).

Annual Exceedance Probability	Recurrence Interval (Years)	Peak Discharge (cfs)
0.50	2	3,010
0.10	10	5,250
0.04	25	6,510
0.02	50	7,520
0.01	100	8,550
0.02	500	11,130

HYDRAULIC MODEL DEVELOPMENT

Steady state, water surface profiles of the Upper Sandy River were simulated with a hydraulic model developed using the U. S. Army Corps of Engineers Hydraulic Engineering Center River Analysis System (HEC-RAS), version 4.1.0. The baseline model was based on an existing HEC-RAS model developed by STARR (2013) for the Oregon Department of Geology and Mineral Industries as part of recent efforts to update flood hazard maps for the Sandy River. For the present study, NSD used the reach geometry for the segment upstream of the Zigzag River confluence and evaluated hydraulic parameters for subreaches covering the existing bridge crossing at E. Lolo Pass Road (RM 43.7) and a proposed alternative bridge crossing upstream near RM 44.7.

HEC-RAS iteratively solves for a 1-dimensional (1D) energy equation to attain an energy balance between successive cross-sections along the study reach. The energy equation is:

$$Z_2 + Y_2 + \frac{\alpha_2 V_2^2}{2g} = Z_1 + Y_1 + \frac{\alpha_1 V_1^2}{2g} + h_e \tag{1}$$

where:

Z_1, Z_2 = elevation of the main channel inverts;
V_1, V_2 = average velocities (total discharge/total flow area);
α_1, α_2 = velocity weighting coefficients;
g = gravitational acceleration; and
h_e = energy head loss.

The energy head loss (h_e) between cross-sections is the sum of friction losses and contraction and expansion loss. The equation for energy head loss is written as:

$$h_e = LS_f + C\left|\frac{\alpha_2 V_2^2}{2g} - \frac{\alpha_1 V_1^2}{2g}\right| \tag{2}$$

where:

L = discharge weighted reach length;
S_f = representative friction slope; and
C = expansion or contraction coefficient.

The friction slope between successive cross-sections is derived from a form of Manning's equation written as:

$$Q = \frac{1.49}{n} A R^{\frac{2}{3}} S_f^{\frac{1}{2}} \tag{3}$$

where:

Q = discharge;
A = flow area; and
R = hydraulic radius (area/wetted perimeter);
S_f = friction slope (energy gradient); and
n = Manning's roughness coefficient;

The river schematic and cross-section layout is shown in the attached hydraulic map series. The river is modeled as a single reach for through most of the project area with cross-sections spanning the valley bottom. There is a segment just upstream of the proposed bridge crossing; however, that is set up as a split flow reach at the location of a recent avulsion that occurred in January 2011 between RM 44.8 and RM 44.9. The primary channel currently follows the left-most (southern) fork along a shorter and steeper alignment. The right-most (northern) fork was abandoned during the channel avulsion but still conveys flow during flood events. The relative distribution of flows between the two channels is optimized in the model to balance energy losses across the junction.

Model geometry integrates topographic survey data collected in 2012 for the active channel area with elevations from a 2011 LiDAR-based Digital Elevation Model (DEM) covering the overbank areas. Boundary resistance is estimated by Manning's roughness coefficient (n) with values in the main channel ranging between 0.05 and 0.06 and n-values of vegetated overbank areas between 0.10 and 0.12. STARR (2013) had performed an initial calibration of channel roughness to best fit with direct measurement of stage-discharge relationships from the USGS gaging station below the Salmon River near Brightwood (#14136500; active 2007-2011). No direct measurements of water surface elevation have been reported in the project area for use in model calibration.

BASELINE HYDRAULIC PARAMETERS

FLOOD INUNDATION

Water surface profiles for flood discharges ranging between the 2-year and 500-year recurrence interval flows (Figure 17) were processed using GIS tools in the HEC-GeoRAS extension for ArcGIS to map floodplain inundation in the project area. The simulated water surface elevations were overlaid with the channel and floodplain topography represented in the 2011 LiDAR DEM to calculate variations of water depth in the floodplain areas.

Results are shown in the attached hydraulic map series. The inundation map showing depth for the 2-year recurrence interval flood (3,100 cfs) shows flows that are filling the channel above bank full stage in many locations and beginning to inundate low lying portions of the floodplain and activate side channels. As flows increase to more extreme discharges, lower terraces and additional abandoned channel features become engaged.

Downstream of the Lolo Pass Road Bridge near RM 43.7, flows up to the 500-year recurrence interval flood remain confined in a narrow valley segment. The segment upstream of the bridge remains moderately confined and has a floodplain width ranging between 200 and 400 feet (Figure 18). Clear Creek parallels the Sandy River in this segment but is separated by a Lahar terrace that is 3 to 4 feet higher than the simulated water surface elevation of the 100-year flood. The channel abuts the roadway at meander bends near RM 43.8 and 44.1; both sites of recent bank protection efforts that have hardened the right bank with rock and wood to reduce erosion hazards. Model output shows flood inundation of an abandoned channel feature between the

two recent project sites (RM 43.9-44) that highlights potential risk for future erosion hazards along the roadway. Simulations predict overtopping of Lolo Pass Road near RM 44 at the 100-year flood event or greater.

The floodplain widens further upstream and includes a network of abandoned channel features between the Sandy River and Lolo Pass Road. The abandoned meander loop between RM 44.3 and 44.5 (active channel in the 1970s) backwaters near RM 44.3 at the 2-year flow and is connected at both upstream and downstream ends during the 10-year flood or greater. An older channel feature parallels the Sandy River upstream from RM 44,4 to 44.7. Downstream portions of this old channel are at relatively low elevation and likely inundated by overbank flows from the Sandy River during large floods (Figure 19). The abandoned channel to the north of the Sandy River steepens slightly upstream of RM 44.5 and the upper 500 feet between RM 44.6 and 44.7 appears to have filled in with sediment and is less defined. Cross-section CT traverses this upper segment showing the invert elevation of the abandoned channel is approximately 3 feet higher than the simulated water surface elevation for the 100-year flood (Figure 20).

The cross-section shown in Figure 20 corresponds closely to the proposed alternative access alignment identified in the Reconnaissance Report by David Evans and Associates (2014) between RM 44.6 and 44.7. The floodplain is relatively narrow at this location (175 feet wide) and the simulated water surface elevation during a 100-year flood is confined by terrace surfaces on both sides. The right bank terrace is approximately 2 feet higher than the simulated 100-year flood and only 1 foot higher than the simulated 500-year event. Both simulations of water surface profiles assume a fixed channel geometry (no sedimentation or erosion) and no substantial blockages by wood or debris during flood flows. The alluvial materials that underlie the terrace are erodible as shown by the approximately 80 feet of bank erosion towards the north in January 2011 near RM 44.6 (Figure 20).

The channel segment upstream of the proposed alternative crossing has been more dynamic in response to historical flood events and the floodplain width increases to approximately 460 feet just upstream of RM 44.7 (150% wider than the section downstream at RM 44.6). Upstream from the broad floodplain area at RM 44.7, the channel splits into two distinct flow paths as a result of a recent avulsion between RM 44.8 and 44.9 in 2011. Prior to the avulsion, most of the flow in the main stem Sandy River meandered along the northern flow path. Following the 2011 avulsion and corresponding incision in the southern flow path, the channel now makes a more direct and steeper path through this segment, limiting flood inundation in the former channel (northern flow path) to flood discharges with a recurrence interval of 2-years or greater.

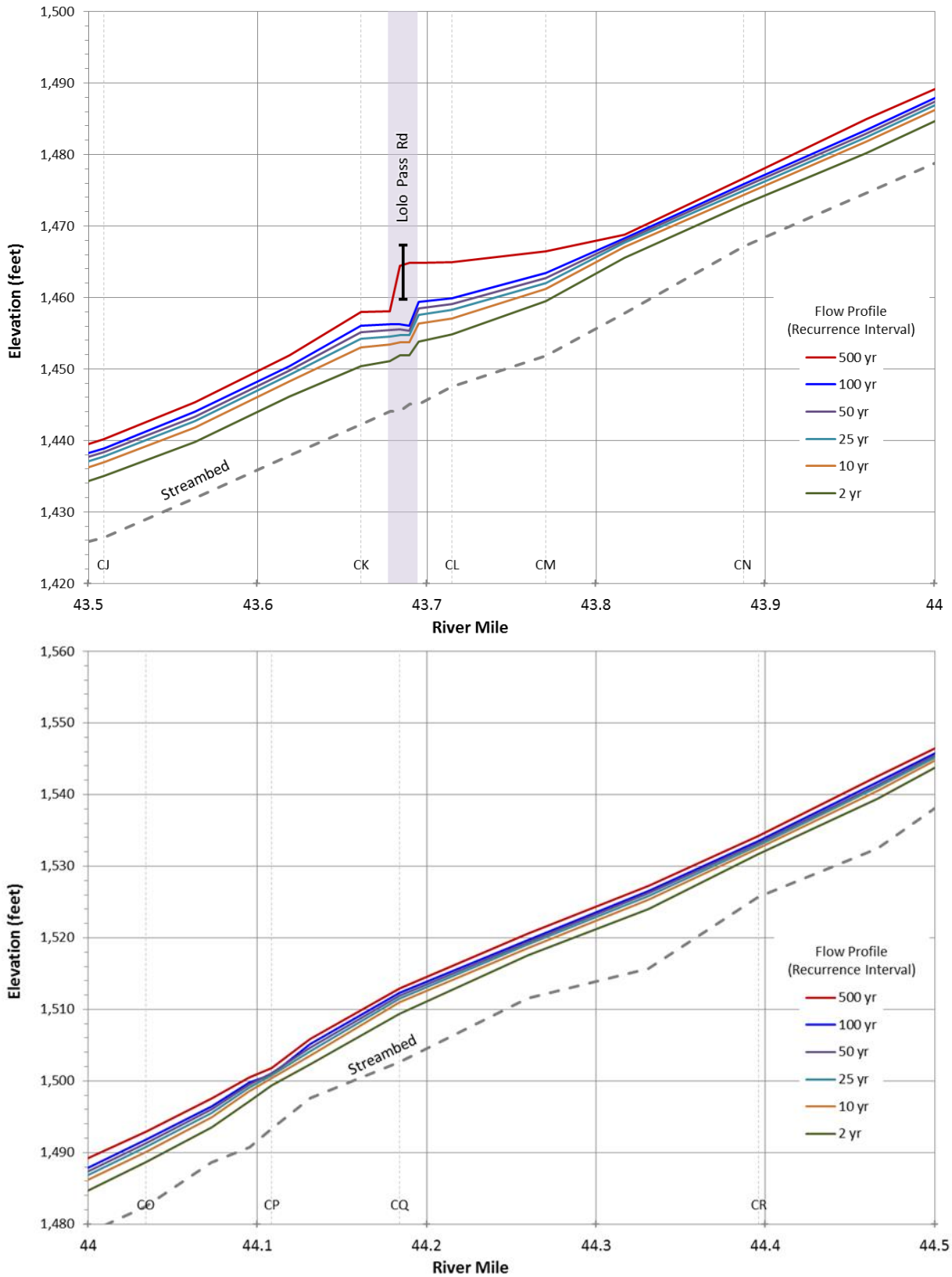

Figure 17. Water surface profiles derived from baseline hydraulic simulations of the Sandy River between RM 43.5 and 44 including the existing bridge at Lolo Pass Road near RM 43.7.

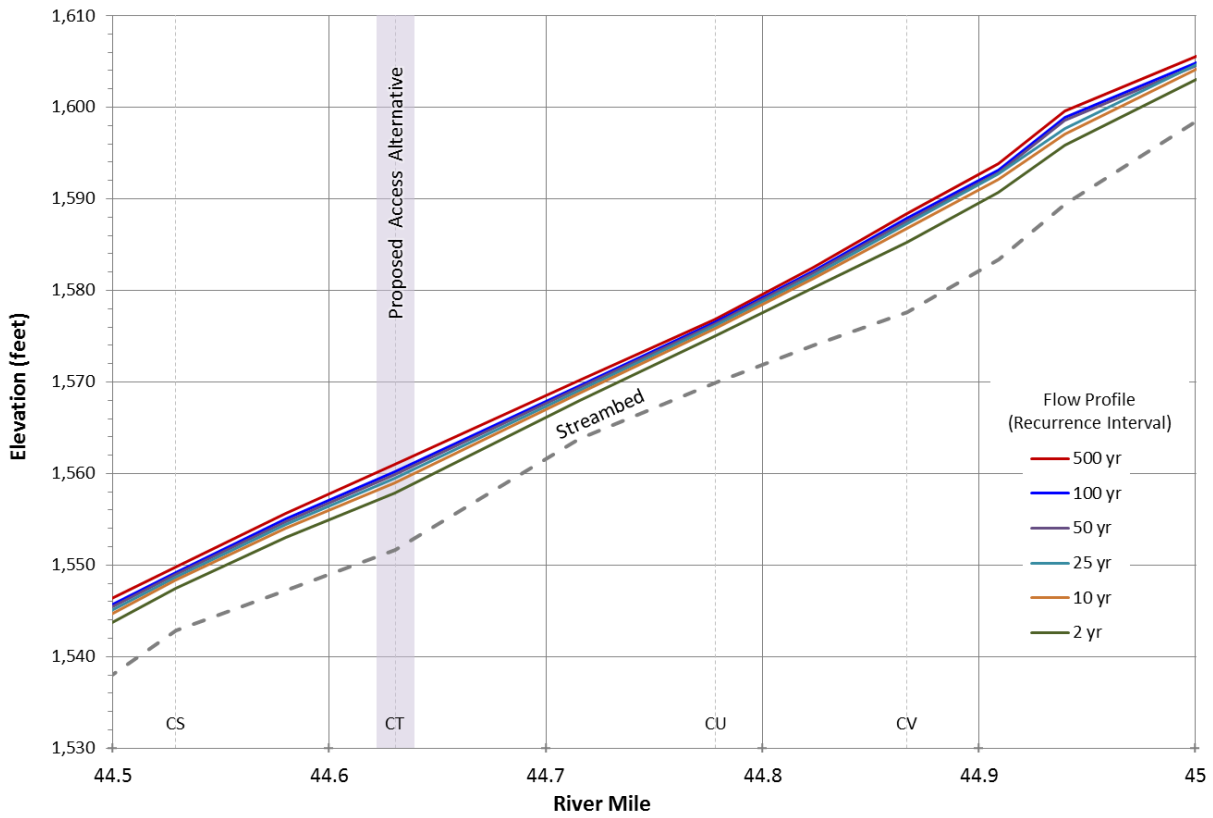

Figure 17 (continued). Water surface profiles derived from baseline hydraulic simulations of the Sandy River between RM 44 and 45 including the proposed access alternative crossing at RM 44.6.

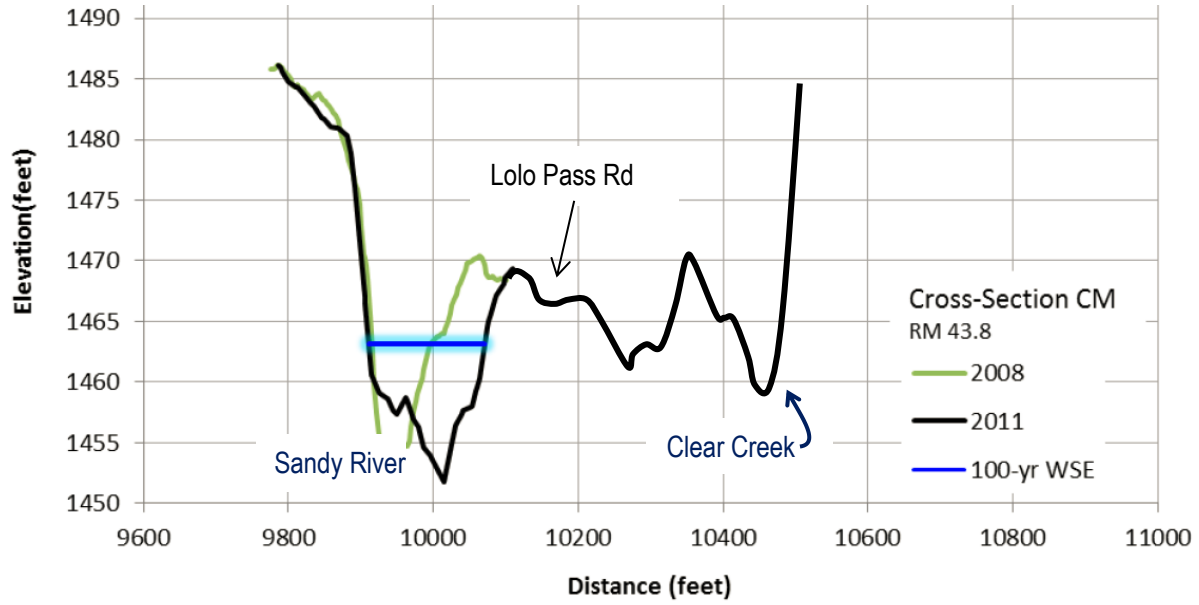

Figure 18. Cross-section CM near RM 43.8 with the simulated water surface elevation for the 100-year recurrence interval flood overlain with LiDAR topography from 2008 and 2011. The channel migrated approximately 80 feet toward Lolo Pass Road in 2011 and has since been hardened by rock bank protection

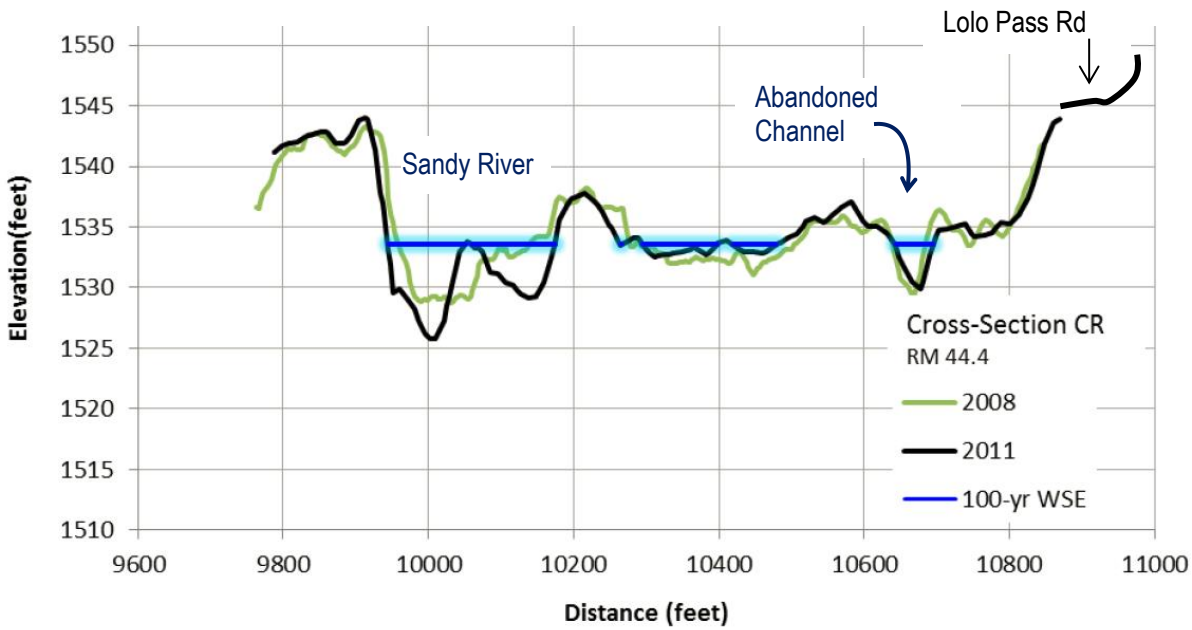

Figure 19. Cross-section CR near RM 44.4 with the simulated water surface elevation for the 100-year recurrence interval flood overlain with LiDAR topography from 2008 and 2011.

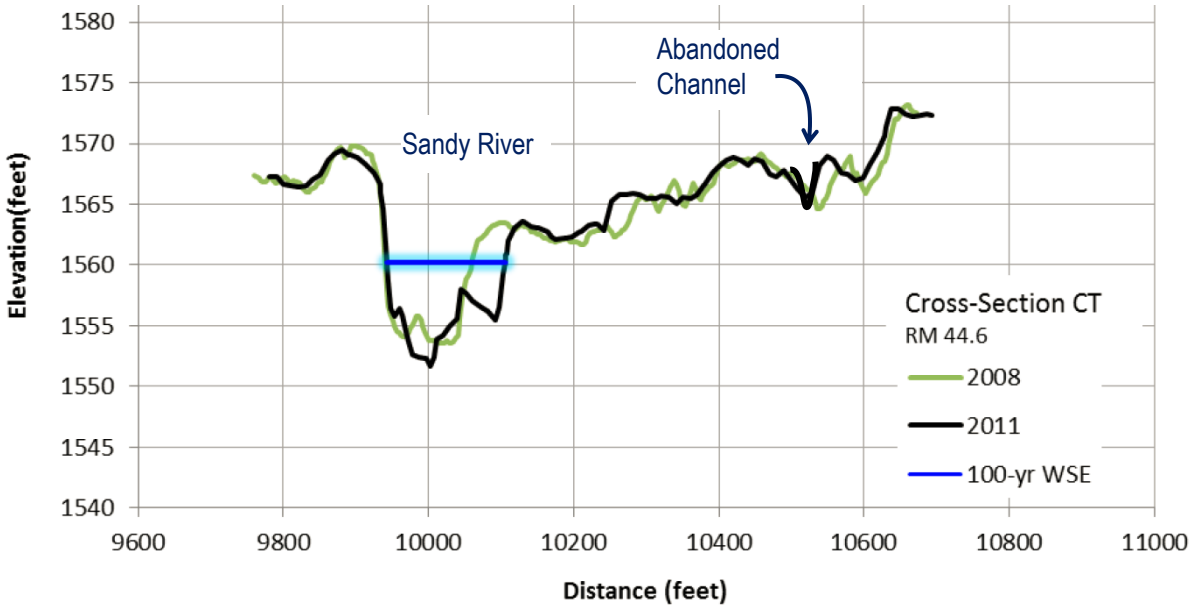

Figure 20. Cross-section CT near RM 44.6 with the simulated water surface elevation for the 100-year recurrence interval flood overlain with LiDAR topography from 2008 and 2011.

VELOCITY AND SHEAR

The velocity of flood discharges is estimated in HEC-RAS using the Manning equation such that:

$$V = \frac{1.49(R^{\frac{2}{3}}S^{\frac{1}{2}})}{n} \quad (4)$$

where:

- V = mean channel velocity;
- R = hydraulic radius (area/wetted perimeter);
- S = friction slope (energy gradient); and
- n = Manning's roughness coefficient.

The slope of the river channel profile is an important control on the flow velocity and exerted stress. The project reach maintains a relatively consistent gradient averaging about 2 percent slope (0.02 ft./ft.) upstream of the existing bridge. There are localized factors along the reach; however, that produce variability in the energy grade line representing the friction slope and the energy available to drive geomorphic processes such as sediment transport and channel migration. The downslope profile of the energy gradient is plotted below in Figure 21. Rapid fluctuations in the energy gradient are observed near the existing bridge as flows are backwatered upstream of the structure and transition through a hydraulic jump immediately upstream of the bridge. Gradient spikes to greater than 3 percent upstream of the bridge near RM 44.1 (cross-section CP) due to a localized steepening of the bed profile and increase in channel confinement relative to the upstream segment. Toe scour in along this bend at RM 44.1 destabilized the embankment causing damage to the roadway in January 2011. Gradient upstream is relatively consistent with the reach average slope between RM 44.4 to 44.8 including the segment proposed as an alternative access alignment for a new bridge. An additional spike in gradient over 3 percent is shown in the approach section to the recent avulsion pathway at RM 44.9.

Mean channel velocity observed in the baseline HEC-RAS simulations follows a similar downstream pattern described for the energy gradient. Velocity of the near-bank full flows represented by the 2-year recurrence interval flood generally range between 6 and 8 feet per second (ft./s) with localized peaks over 10 ft./s.

Extreme floods such as that shown for the 500-year recurrence interval flood average 10 to 12 ft./s with peak values up to 18 ft./s (Figure 22). Note that HEC-RAS is a cross-sectionally averaged, 1D hydraulic model and the results are presented for mean channel velocity. Localized accelerations of flow should be expected within a given cross-section (such as the outside of channel bends) resulting in maximum velocities that exceed the cross-section average.

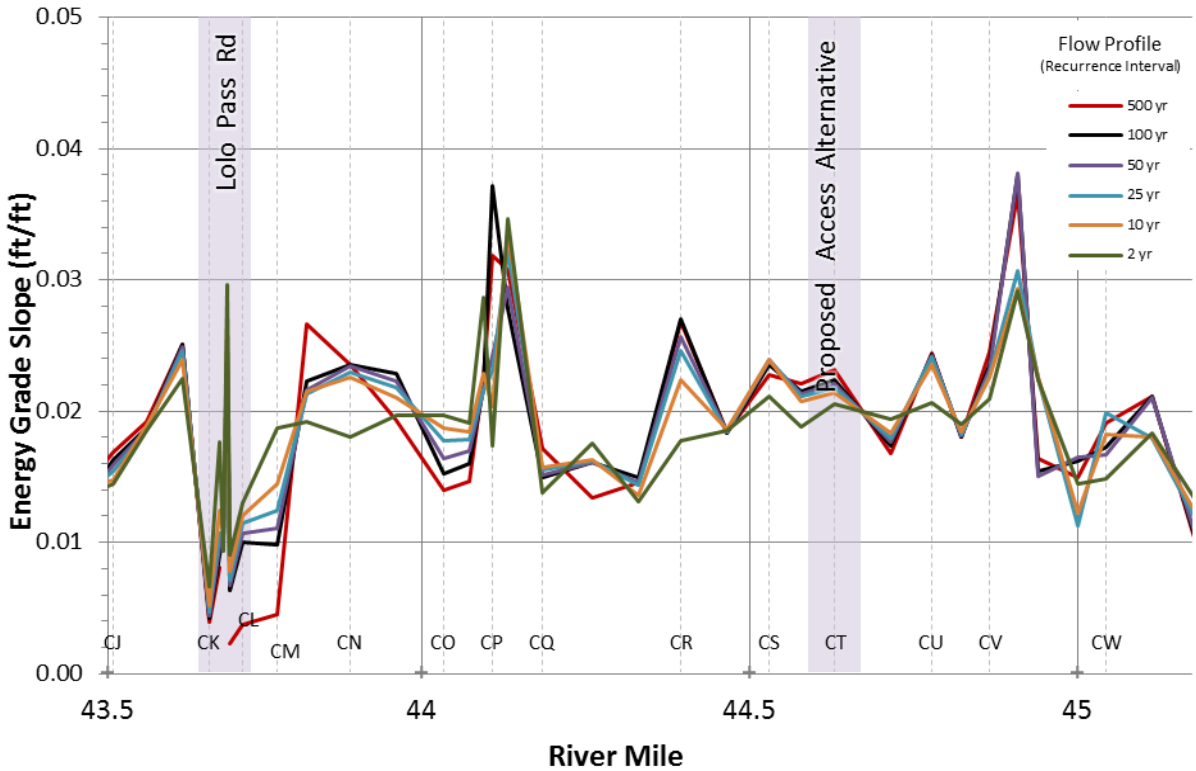

Figure 21. Profile of the energy grade slope derived from baseline hydraulic simulations.

Figure 23 presents a profile of the mean boundary shear stress derived from model simulations. The total applied shear stress at a given flow is the force exerted by the flowing water per unit area of the bed and, assuming the condition of steady, uniform flow, is calculated as:

$$\tau_0 = \gamma R S \quad \textbf{(5)}$$

where:

τ_0 = total shear stress (lb/ft^2)
γ = specific weight of water (lb/ft^3)
R = hydraulic radius (ft.)
S = energy slope (ft./ft.)

The mean boundary shear stress calculated in HEC-RAS simulations averages between 3 to 4 pounds per square foot (lbs/ft^2) for the 2-year recurrence interval flood and increases to 6 to 8 lbs/ft^2 during more extreme flows such as the 500-year event (Figure 23). Peak shear stress values up to 16 lbs/ft^2 were predicted. Channel segments characterized by extreme shear stress values generally correspond to sub-reach areas with localized increase in gradient or channel confinement.

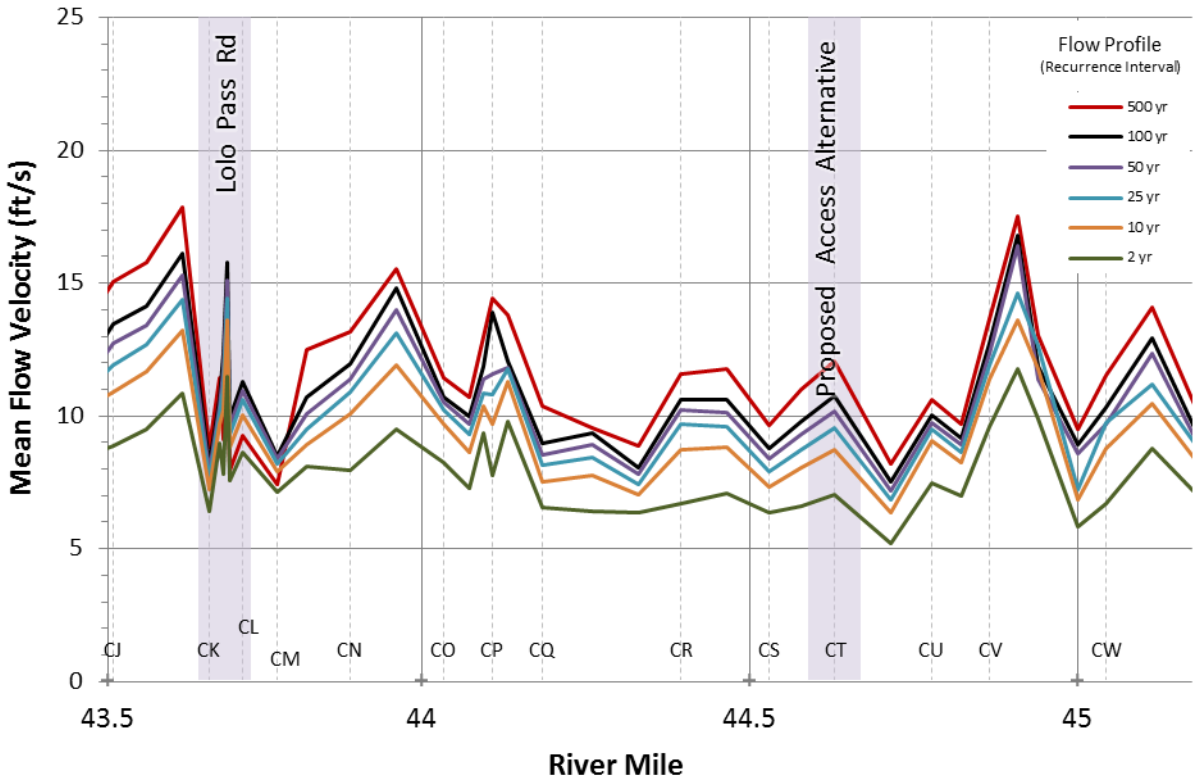

Figure 22. Profile of the mean flow velocity derived from baseline hydraulic simulations.

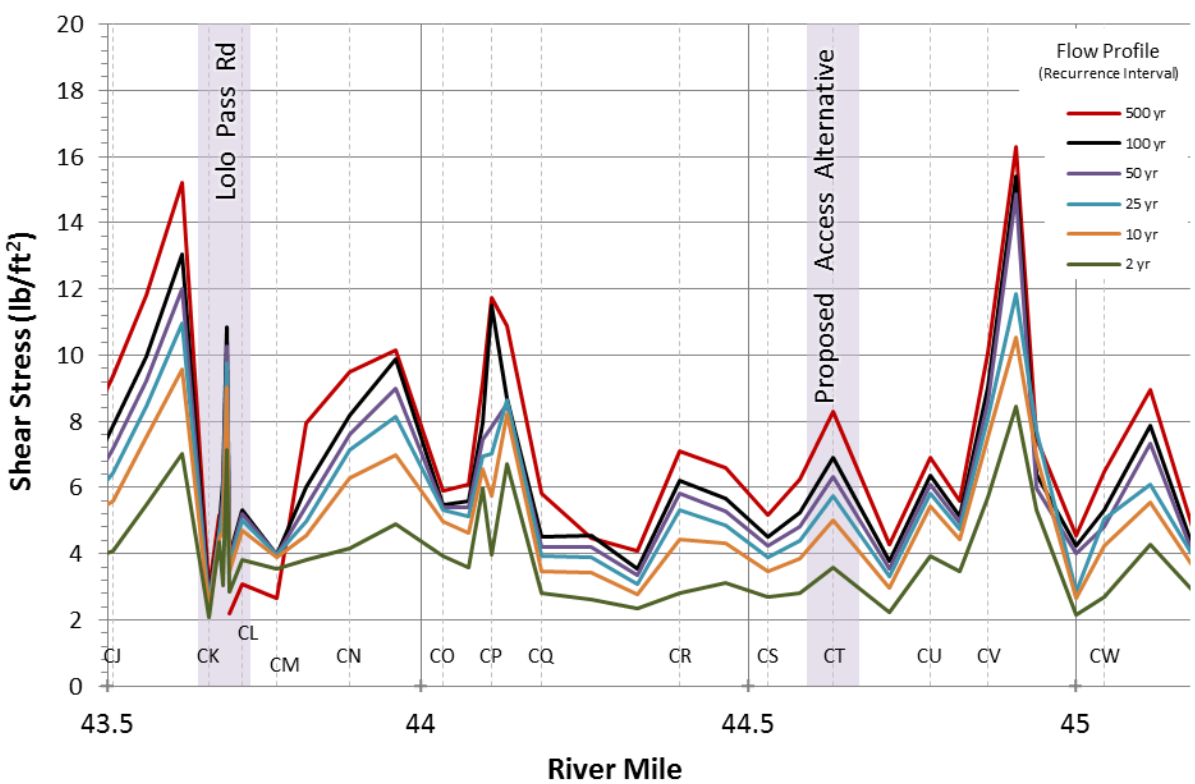

Figure 23. Profile of the mean boundary shear stress derived from baseline hydraulic simulations.

SEDIMENT TRANSPORT POTENTIAL

Erodible sediment grains on the channel bed are entrained by flow when the grain stress, τ_{gs}, exceeds the critical shear stress for grain motion ($\tau_{gs} > \tau_c$). The critical shear stress for grain motion is derived using a function of the sediment grain size and calculated by a relation developed by Shields (1936) such that:

$$\tau_c = \tau_c^*(s-1)\rho g D \quad \textbf{(6)}$$

where:

τ_c = critical shear stress (lb/ft^2)
τ_c^* = Shields parameter
s = specific gravity of sediment
ρ =density of water (lb/ft^3)
g = constant for the acceleration due to gravity (ft./s^2)
D = grain size diameter (ft.)

An approach by Wilcock et al. (2009) approximating the original Shields curve to was followed to estimate the Shields parameter by the function:

$$\tau_c^* = 0.105{S^*}^{-0.3} + 0.045e^{-35{S^*}^{-0.59}} \quad \textbf{(7)}$$

where:

S* = dimensionless viscosity

Reference values of critical shear stress for a range of grain size classifications using Wilcock et al.'s (2009) approximation of the Shields curve described in Equations (6) and (7) are summarized below in Table 4.

NSD collected pebble count samples of bed material sediment during fieldwork completed in 2014 as part of an Erosion Hazard Assessment prepared for Clackamas County. The sample location near RM 44.9 is approximately 1,500 feet upstream of the proposed alternative access alignment identified by David Evans and Associates Inc. (2014). Two samples were recorded at this location to characterize the cobble-dominated coarse grained material observed in the main channel and a finer grained, gravel-dominated substrate observed in depositional areas on bar surfaces (Figure 24).

Comparison of the total applied shear stress calculated in HEC-RAS simulations (Figure 23) with the estimated critical shear stress values summarized in Table 4 highlights the extremely high potential for sediment mobility during flood events. Using just the average shear stress during a 2-year recurrence interval flow (around 3 lbs/ft^2) predicts entrainment of cobble sized bed material. Higher shear stress values observed in localized areas far exceed the critical shear stress values required for entrainment of boulder-sized particles.

Estimates of the sediment transport rate for a given channel can be defined by a power function of the difference between the bed shear stress and the critical shear stress for grain motion such as:

$$q_b = k(\tau_{gs} - \tau_c)^n \quad (8)$$

where:

q_b = bedload transport capacity (lb/ft^2)

τ_{gs} = grain stress (lb/ft^3)

τ_c = critical shear stress for grain motion

n and k are empirical constants

The grain stress referenced in (8) represents that portion of the total applied shear stress that acts on the erodible sediment grains and drives sediment transport. The grain stress, τ_{GS}, is a component of the total applied shear stress. The process of separating the total shear stress into the grain stress and additional components representing other sources of hydraulic resistance is referred to as stress partitioning (Einstein and Barbarossa, 1952). In plane bed channels that lack bed forms and wood, we assume that the primary source of hydraulic resistance is due to the sediment grains and that grain stress is the primary component of the total applied shear stress ($\tau_{gs} \approx \tau_0$). In other channel types with more hydraulic and geomorphic complexity, grain stress can be a much smaller component of the total applied shear stress ($\tau_{gs} < \tau_0$). Manga and Kirchner (2000), for example, used field measurements to partition shear stress and determine the relative contribution of wood to the reach-average total shear stress for a spring-fed river with relatively constant discharge. Manga and Kirchner (2000) demonstrated that wood covering less than 2% of the streambed in the study reach accounted for up to 50% of the total flow resistance in the study reach.

Key points to derive from equation (8) are that sediment transport rates are a nonlinear function of excess shear stress and that downstream variations will be expected due to localized differences in stress partitioning that are most closely associated with quantities of wood loading. In summary, sediment transport potential in the Upper Sandy River is extremely high, as seen in the geomorphic response to recent flood events, but local variation associated with wood loading can reduce transport capacity in local areas.

Table 4. Estimated Shields parameter (τ_c^*) and critical shear stress (τ_c) values derived from Equations (6) and (7) for a range of sediment grain sizes.

Sediment Classification	D (mm) (upper limit)	τ_c^*	τ_c (lb/ft^2)
boulder	512	0.046	8.0
large cobble	256	0.046	4.0
small cobble	128	0.047	2.0
very coarse gravel	64	0.047	1.0
coarse gravel	32	0.046	0.50
medium gravel	16	0.045	0.24
fine gravel	8	0.042	0.11
very fine gravel	4	0.038	0.05
very coarse sand	2	0.033	0.02
coarse sand	1	0.031	0.01
medium sand	0.5	0.035	0.006
fine sand	0.25	0.046	0.004
very fine sand	0.125	0.063	0.003

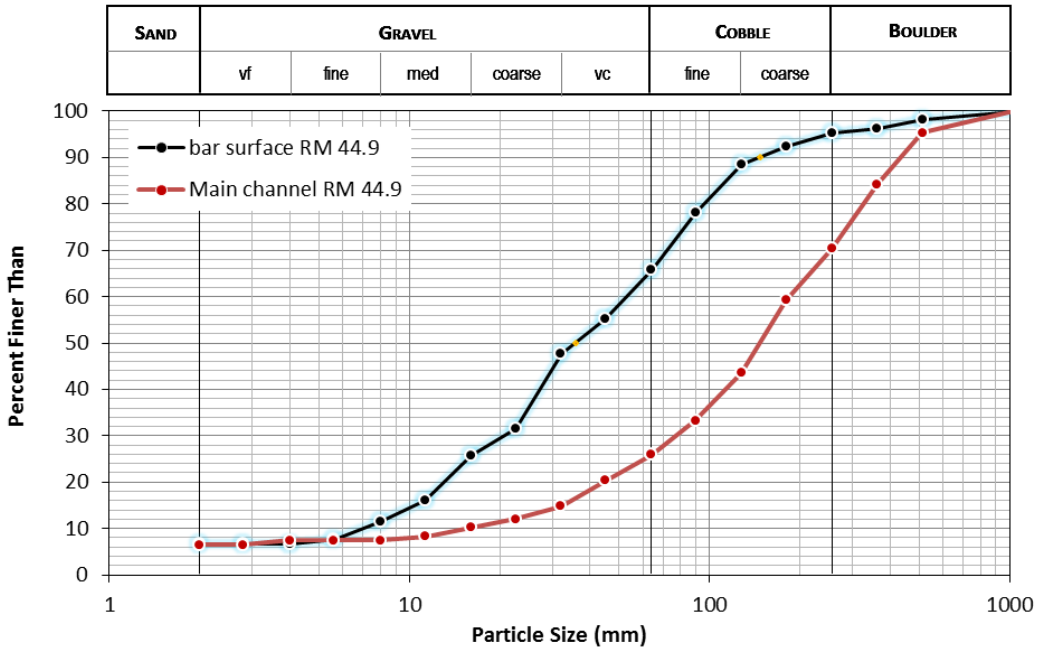

Figure 24. Grain size distribution of pebble count samples near RM 44.9. Median grain diameter (D_{50}) in the main channel is 146 mm (large cobble) whereas deposition on the bar surface has a D_{50} of 36 mm (coarse gravel). Photo shows the existing main channel (2011 avulsion pathway) on the left and bar surface within the abandoned channel area to the right.

BRIDGE CROSSING EVALUATION

EXISTING BRIDGE CROSSING AT LOLO PASS ROAD (RM 43.7)

The bridge crossing the Sandy River at Lolo Pass Road was reconstructed in 1965 following damages resulting from the December 1964 flood. The bridge has a span length of 80 feet that is supported by vertical concrete abutments with wing walls (Figure 25). Accounting for the bridge skew angle of 30°; however, the projected width of the bridge opening normal to flow is reduced to 70 feet. The low chord of the bridge is at an elevation of 1459.6 feet and approximately 14.5 feet above the channel thalweg at the cross-section upstream of the bridge.

The segment upstream of the bridge is confined by high banks. The 1964 flood triggered rapid erosion towards Lolo Pass Road and avulsion of the main channel that washed out the bridge abutments (Figure 26). The channel was re-aligned and the banks were regraded in 1965 with construction of the new bridge. Scour during recent floods has undermined the high banks in places such as the meander bend 500 feet upstream where a rock revetment was constructed in 2011 to stabilize an eroding bank adjacent to Lolo Pass Road. Further upstream near RM 44.1 the road was completely washed out by erosion in 2011.

Hydraulic parameters of the existing bridge crossing were evaluated from simulation s in HEC-RAS. The model calculates energy losses associated with the bridge structure using a series of four cross-sections. Sections immediately upstream and downstream of the bridge opening are drawn parallel to the road alignment (Figure 26). The bridge skew angle is applied to correct the cross-sectional geometry and project channel width normal to the flow. Ineffective flow areas are designated outside of the bridge opening to identify areas of the cross-section not actively conveying flow. Two additional cross-sections are utilized to define the upstream and downstream ends of the contraction and expansion zones, respectively.

The bridge modeling approach varies with flow stage. During flow conditions for which the water surface is below the below the low chord of the bridge, the energy method is applied to calculate energy losses. Flows at recurrence intervals between 2- and 100-years were all evaluated using the energy method. As flow stage increases and the water surface comes into contact with the low chord of the bridge, the pressure and weir flow is generally applied. The pressure/weir method is assumed valid for conditions in which:

$$\frac{Y_a}{Z} > 1.2 \tag{9}$$

where:

Y_a = hydraulic depth at the cross-section upstream of the bridge opening; and

Z = vertical distance between the low chord of the bridge opening.

For the bridge crossing at E. Lolo Pass Rd., the above relation was only valid for flows the 500-year event. Pressure flow was calculated using a submerged inlet and outlet coefficient of 0.8 and a weir coefficient of 2.6.

Figure 25. Photo looking upstream at the Lolo Pass Road bridge crossing the Sandy River near RM 43.7.

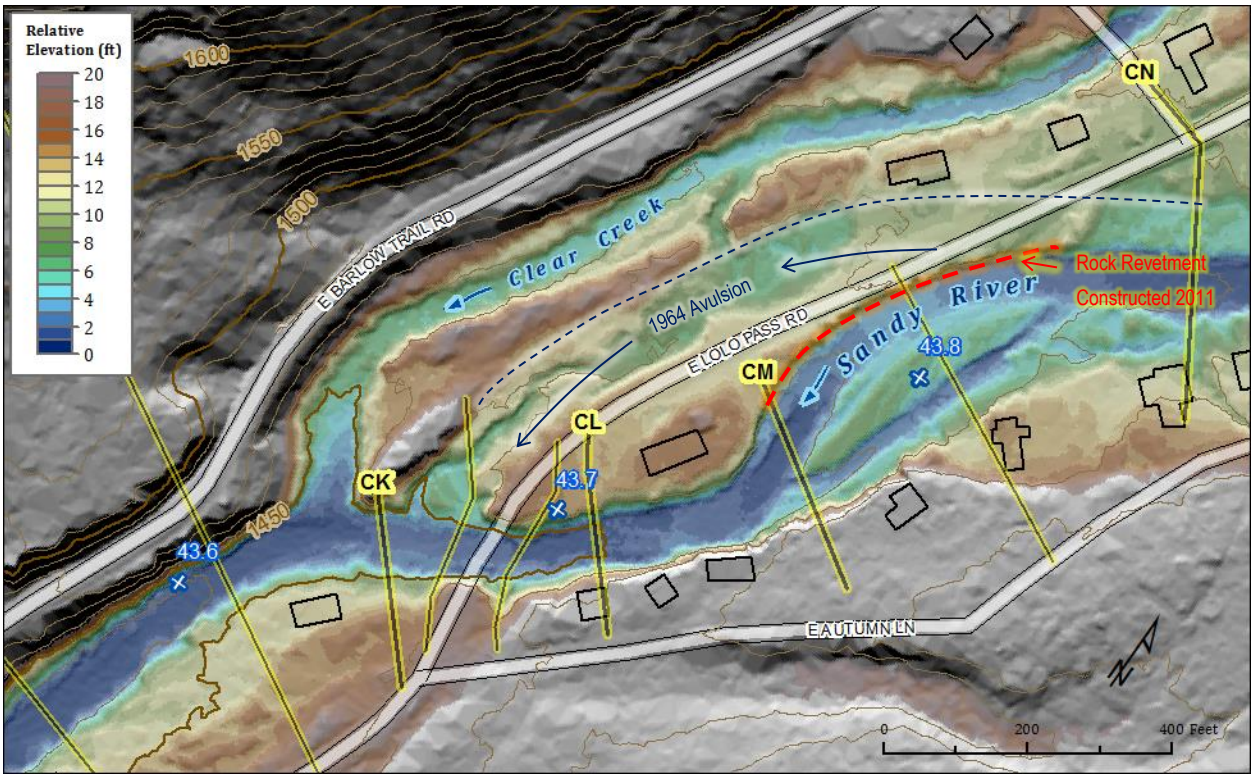

Figure 26. Relative elevation map of the existing bridge crossing the Sandy River at Lolo Pass Road near RM 43.7. Topography is derived from 2011 LiDAR data.

Water surface profiles through the bridge crossing at E. Lolo Pass Road are shown in Figure 22. The profiles for flow recurrence intervals up to the 100-year flood pass within the bridge opening. Water surface is generally backwatered upstream and then transitions through a hydraulic drop to supercritical flow at the upstream cross-section for the bridge. The constriction results in a spike of velocity over 15 feet per second and basal shear stress over 10 pounds per square feet for the 100-year flood. There is a hydraulic jump as flow transitions to subcritical on the downstream side of the bridge. Transitions between sub- and supercritical flow are associated with extreme turbulence that can exacerbate scour and increase erosion hazards at bridge crossings.

The simulation of the 500-year flood resulted in a high flow condition with both inlet and outlet submerged. Although the water surface of the 500-year event is approximately 5 feet above the low chord of the bridge opening, only 3 percent of the total flow crosses over the roadway as weir flow. Nearly all of the flow is crossing through the bridge opening as pressure flow. All profiles simulated in the model produce a backwater effect in the channel segment extending 400 to 600 feet upstream of the bridge (Figure).

WIDENED BRIDGE SPAN AT EXISTING CROSSING

Based on observations from historical channel migration and evaluation of baseline hydraulic parameters, an alternative scenario was evaluated to consider the hydraulic effects of a wider bridge span at the existing road crossing location. Conceptual design criteria in this evaluation included: (1) increasing flow conveyance through the approach segment with a wider channel and setback bank protection; (2) replacing the existing bridge and abutments with a new structure with two 200-foot bridges; and (3) moving the alignment of Lolo Pass Road approximately 200 feet north to the edge of the bankline formed during the 1964 flood (Figure 27). Figure 28 shows a cross-sectional schematic of the conceptual bridge crossing with a 200-foot span.

Hydraulic parameters of the conceptual alternative scenario were evaluated with modifications to the river geometry in HEC-RAS. Assuming that design of the approach section upstream of the bridge includes expansion of the channel cross-section to address the present constriction, the net effect of the increased flow conveyance is a 1.9 foot reduction in water surface elevation, 57 percent decrease in flow velocity, and 81 percent decrease in total applied shear stress driven by the 100-year flood (Table 5). Note that even with predicted moderation of velocity and shear, erosion hazards will continue to threaten Lolo Pass Road as it parallels the Sandy River within the Channel Migration Zone and a considerable longer span (or series of spans) will likely be required to accommodate geomorphic processes: (bed aggradation, channel migration).

Evaluation of potential impacts to other property and infrastructure should consider how modifications in channel geometry affect the angle of flowlines through the reach and the distribution of shear stress along the channel boundary. The present configuration has a meander bend upstream of the bridge that has required armoring with a riprap revetment to protect the road. This right bank revetment directs flow towards the opposite (left) bank downstream and erosional forces are concentrated on this left bank along Autumn Lane just

upstream of the bridge. The design alternative that widens the existing span will better accommodate future channel adjustments and lateral migration; however, as the channel migrates, the areas of concentrated shear stress will change over time. It is unlikely that such changes will adversely affect the left bank properties along Autumn Lane as these parcels are already at high risk for erosion hazards. There is potential to adversely affect the property just downstream of the bridge, however, because the current channel pattern directs flow through the bridge and concentrates shear stress on the opposite (right) bank. Enabling a more dynamic channel network through this segment could increase the probability that shear stress is concentrated along the left bank and accelerate erosion along the left bank private property. These impacts are limited to a localized area around the existing bridge and likely only affecting an area approximately 500 feet upstream and downstream of the bridge.

Table 5. Comparison of flow velocity and total applied shear stress for the 100-year recurrence interval flood under existing conditoins (80-foot wide span) and a conceptual alternative scenrio with a 200-foot wide span.

	Existing Conditions 80-ft. Bridge	Future Scenario 200-ft. Bridge
Upstream WSE (ft.)	1459.4	1457.5
Mean Velocity (ft./s)	15.8	6.8
Shear Stress (lb/sq ft.)	10.9	2.1

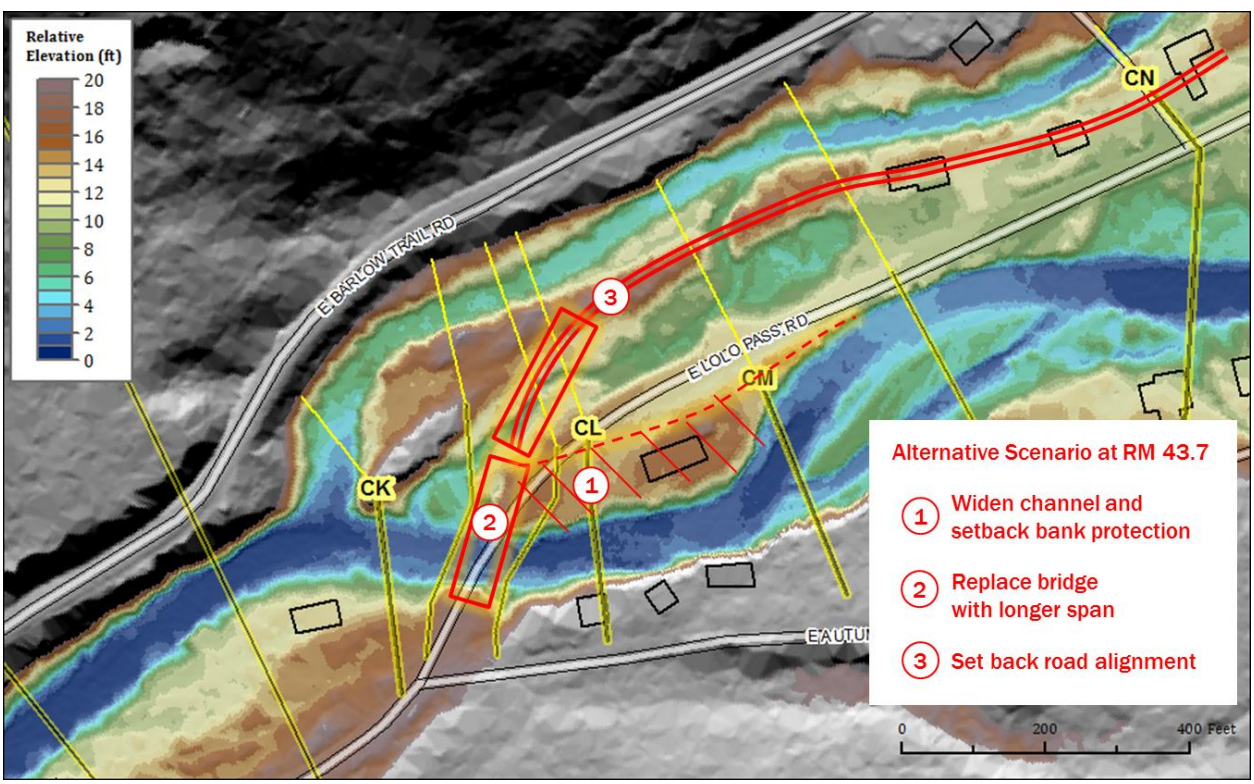

Figure 27. Conceptual sketch of an alternative scenario with a widened bridge crossing (two, 200-foot spans) at the existing road crossing near RM 43.7.

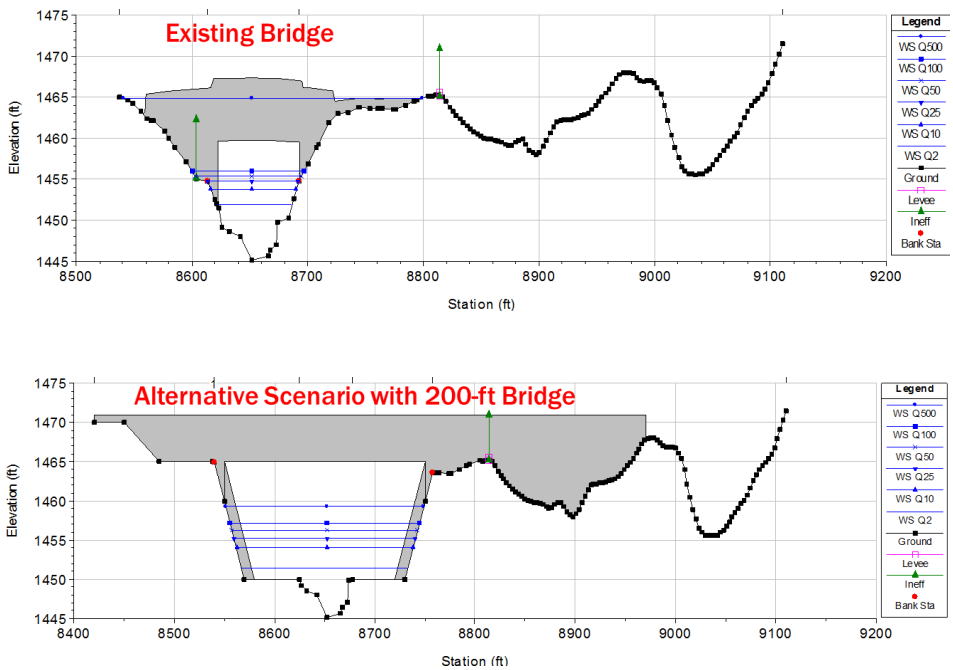

Figure 28. Cross-section at the existing bridge crossing at Lolo Pass Road (RM 43.7) showing the baseline conditions (80-foot span) and a conceptual alternative scenario with a 200 foot wide bridge crossing.

ACCESS ALTERNATIVE NEAR RM 44.7

The 2014 Reconnaissance Report by David Evans and Associates identifies a potential access alternative approximately 1 mile upstream of the existing road crossing near RM 44.7. The route parallels the south side of the Sandy River upstream to the end of Autumn Lane, turns northwesterly across the active channel and valley bottom, then climbs upslope to merge with the existing road alignment on the north side of the valley (Figure 29). The channel migrated approximately 80 to 100 feet towards the right bank at this location in the 2011 flood.

Evaluation of the proposed alternative bridge crossing upstream near RM 44.7 (Figure 29) simulated a series of flows for the baseline conditions as well as two future scenarios representing episodic channel aggradation associated with pulses of sediment delivered from upstream. The two future scenarios applied a uniform bed adjustment of 4 feet and 8 feet, respectively, representing a range of possible channel aggradation associated with large flood events in the Sandy River basin. Aggradation in this range was observed in depositional areas of the project reach at locations where the channel has avulsed during recent floods. Model simulations of potential future scenarios also increased the roughness coefficient of the active channel area by 50% to mimic the hydraulic effect of widespread wood recruitment as observed in past floods such as the 1964 event. The net effect of the geometry modifications with the potential future scenarios yields a conservative estimate of flood hydraulics to guide evaluation of bridge crossing alternatives. An important distinction, however, is that future condition scenarios did not address potential sedimentation associated with lahars that would likely deliver a much greater volume of sediment and pose a substantial risk to local communities.

A summary of the required low chord elevations at the proposed alternative crossing for the three scenarios evaluated is presented in Table 6. In the baseline conditions simulation, note that flood flows are contained within high banks formed of lahar deposits that separate the active channel from an abandoned channel feature in the north side of the valley (Figure 30). A span length approximately 200 feet would likely be sufficient in the baseline scenario for a road crossing near RM 44.7. Much longer crossings are required to pass flood flows under the future conditions scenario (Figure 30). Based on the simulated water surface elevation from the 100-year flood, a span length (or cumulative length from multiple spans) closer to 600 feet is required to pass flood flows without affecting hydraulics of the reach.

In the future condition simulation representing episodic channel aggradation, the water surface profile during more extreme floods (e.g., 100- to 500-year recurrence interval event) begins to overtop the terrace surface upstream of the proposed crossing and drain into the abandoned channel feature. This channel feature should be noted as a substantial channel migration hazard and bridge crossing designs should consider potential for including an additional span to cross the abandoned channel. In this future scenario, the flow entering the abandoned channel would likely lead to downcutting and expansion of the cross-sectional area; thus increasing the likelihood of channel avulsion similar to the avulsion that occurred immediately upstream in January 2011 shifting the active channel to the opposite side of the valley.

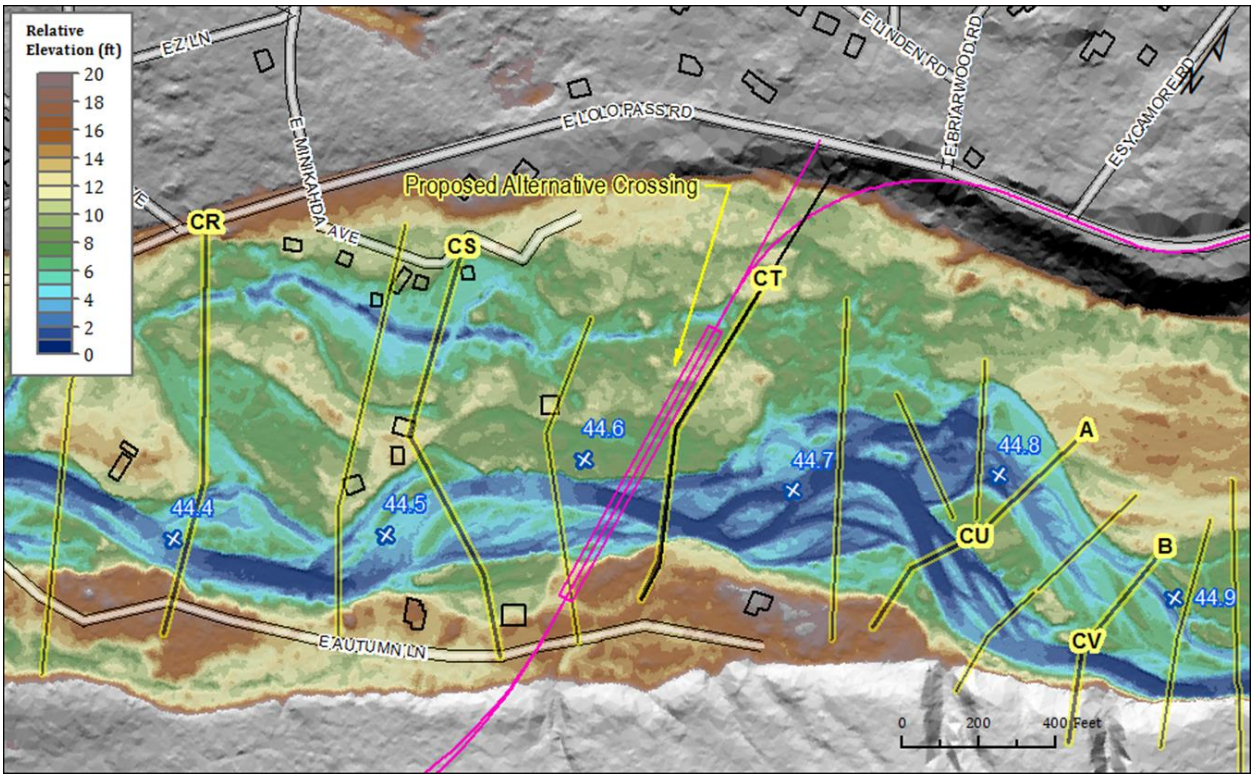

Figure 29. Map of the Upper Sandy River at the proposed alternative bridge crossing near RM 44.7 showing the cross-section layout from the HEC-RAS model and relative ground surface elevations derived from the 2011 LiDAR DEM. The pink line highlights a proposed access alternative alignment developed by David Evans and Associates.

Table 6. Summary of model results at the alternative crossing near RM 44.7.

Scenario	Water Surface Elevation 100-year Flood[1]	Required Low Chord Elevation[2]
Baseline Channel Geometry	1562.0	1565.0
Future Scenario with 4 feet of aggradation	1567.1	1570.1
Future Scenario with 8 feet of aggradation	1568.8	1571.8

[1]NAVD 1988

[2]Assuming 3 feet of freeboard

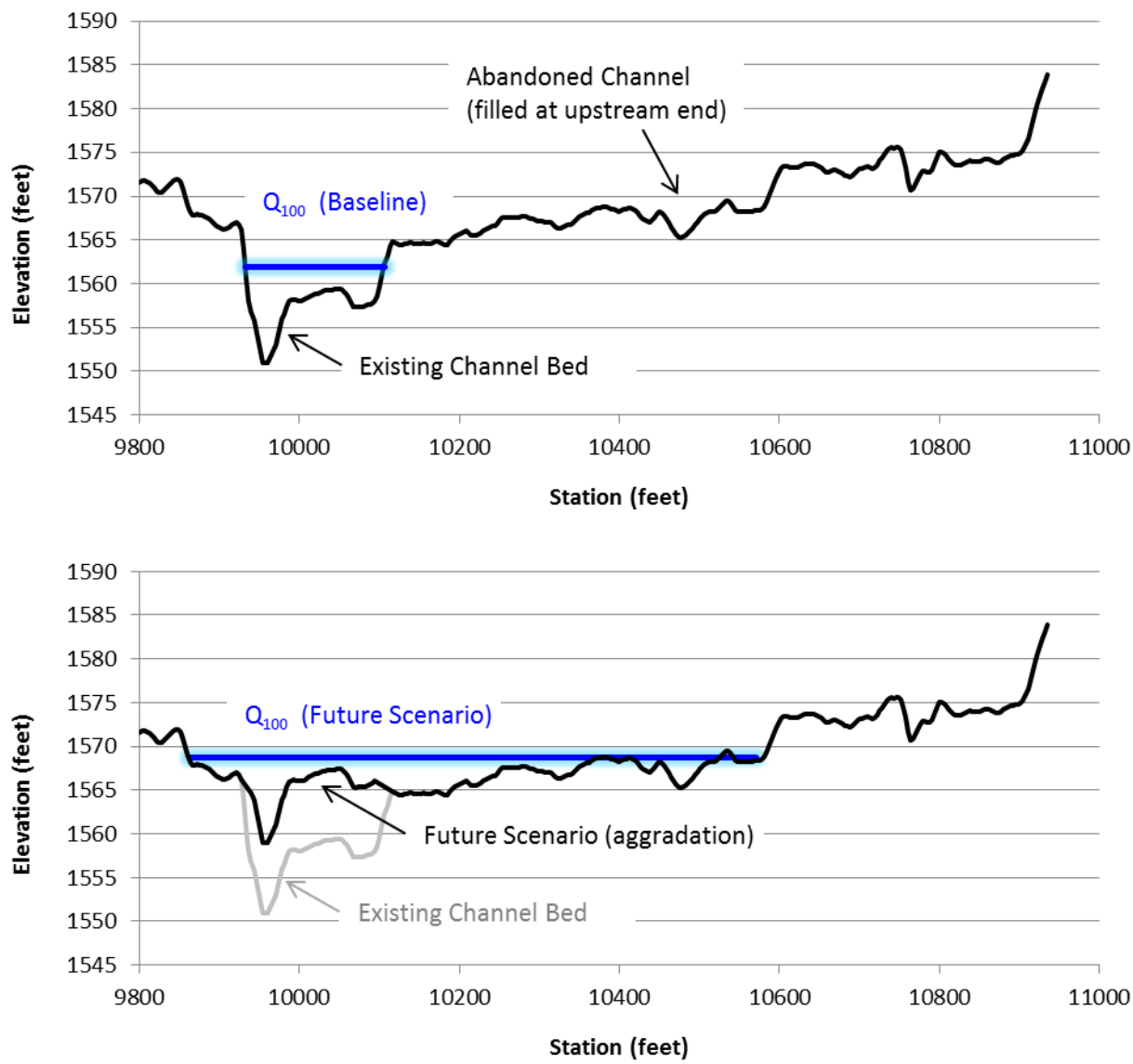

Figure 30. Cross-sectional profile through the proposed alternative bridge crossing near RM 44.7. The upper panel shows the baseline channel geometry and predicted water surface elevation for the 100-year recurrence interval peak discharge (Q_{100}). The lower panel shows the representation of a future scenario with deposition of 8-feet of sediment resulting in aggradation of the active channel and the resulting Q_{100} water surface.

SCOUR ANALYSIS

Bridge scour involves the mobilization of sediment from around the bridge foundation (abutments and/or piers) during flood flows and is the most common cause of bridge failure. This evaluation presents a preliminary assessment of scour to support the Access Alternatives Analysis in preparation by David Evans and Associates.

Alternatives evaluated for this study include:

- No action alternative based on existing conditions;
- A design alternative with two, 200-foot bridge spans to replace the existing crossing (Figure 31); and
- A design alternative to construct an 800-foot bridge (four, 200-foot spans) spanning the river corridor near RM 44.6 (Figure 32).

At this stage in the project, there are not sufficient details to fully quantify the anticipated scour depth of the proposed design alternatives. In particular, further design is required to define criteria for channel modifications in the approach sections upstream of the proposed bridges. The scour analysis described in this evaluation provides a general overview of the primary mechanisms of bridge scour affecting the proposed access alternatives crossing the Sandy River. Additional hydraulic analysis, including calculation of scour depths will be required during the design phase for the selected alternative.

Total scour depth is typically estimated as the sum of three primary components:

- Long-term degradation of the river bed;
- Contraction scour at the bridge; and
- Local scour at bridge piers and abutments.

A fourth consideration to bridge scour and stability in the Upper Sandy River is lateral channel migration.

Proposed bridge geometry of the two design alternatives was provided by David Evans and Associates and entered into the model for proposed alternatives. Scour analyses were based on methods described in the U.S. Department of Transportation Federal Highway Administration (2012) Hydraulic Engineering Circular No. 18 (HEC-18). The scour design discharge selected for evaluation was the 100-year recurrence interval peak flow (Table 3).

LONG TERM DEGRADATION

Channel degradation refers to a long-term erosional trend caused by an imbalance between sediment supply and transport capacity that results in a lowering of the bed elevation over time. Given the dynamic nature of the project reach, rapid fluctuations of the channel bed, both

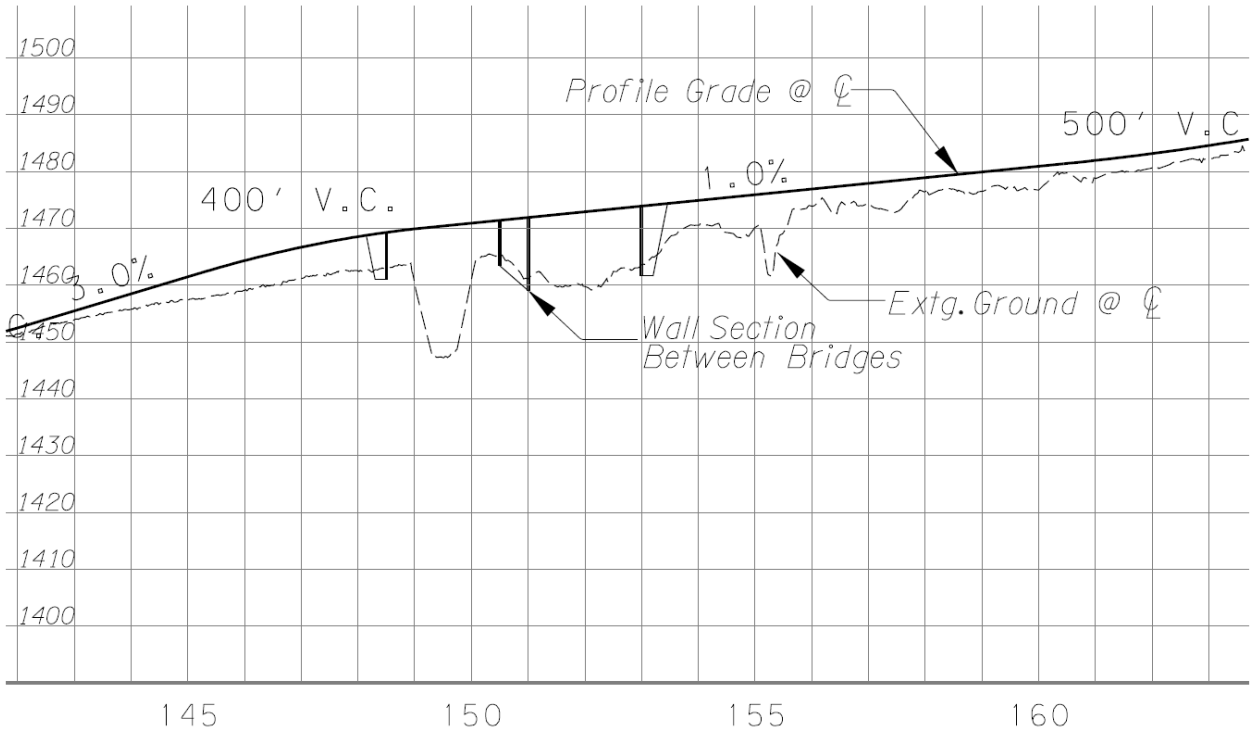

Figure 31. Cross-sectional profile of the proposed design alternative to widen the existing bridge structure with two, 200-foot bridge spans. Source: David Evans and Associates.

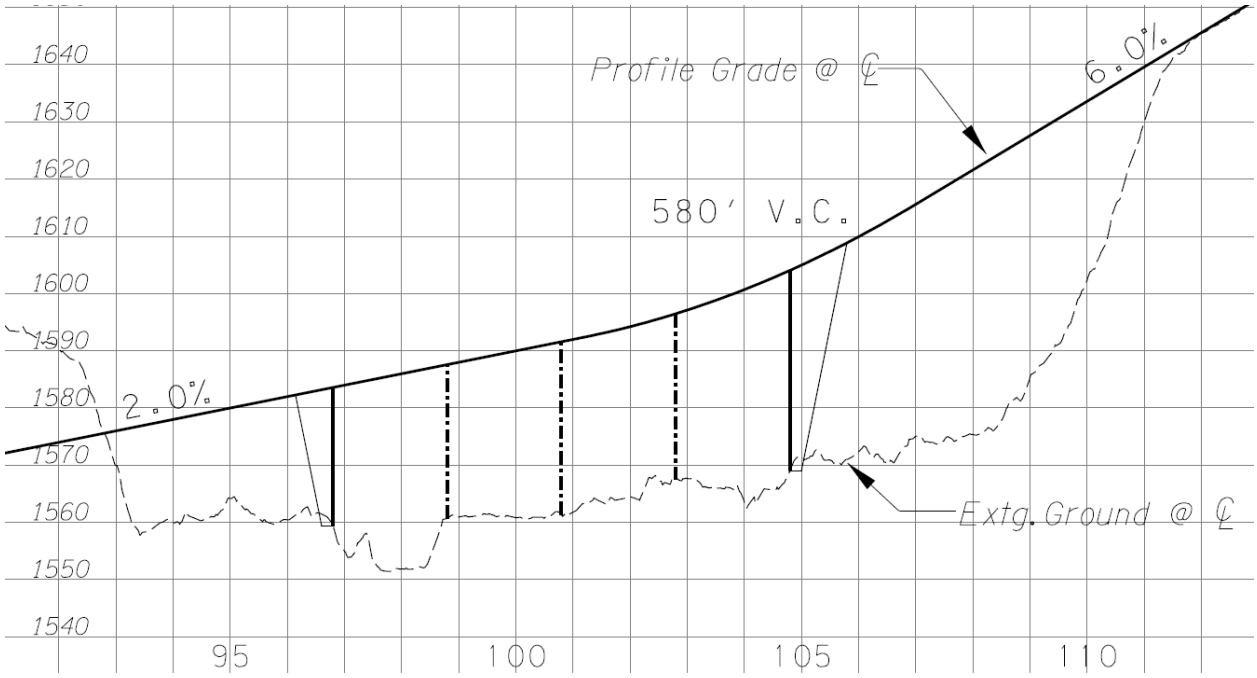

Figure 32. Cross-sectional profile of the proposed design alternative to construct a new 800-foot bridge (four, 200-foot spans) near RM 44.6. Source: David Evans and Associates.

upward and downward, are expected in response to episodic pulses of sediment production from the upper watershed. Although periods of sediment deposition and aggradation are possible, the channel evolution and response to past valley filling lahars suggests that additional lowering of the bed is also expected over time as the channel continues to adjust to past disturbance (Figure 6). For the purpose of scour analysis, potential for long-term degradation was considered to ensure a conservative estimate of scour depth for each alternative scenario. Future degradation potential of up to 6 feet was estimated based on evaluation of the channel migration history and elevation differences between the existing channel and abandoned channel features in the valley representing previous occupation of the Sandy River. This estimate was applied uniformly to all alternative scenarios as a component of the total scour depth. There is a rather high level of uncertainty to this component given the episodic nature of sediment production from geomorphic processes in the upper watershed and the lack of historical elevation data to quantify vertical channel changes.

CONTRACTION SCOUR

Contraction scour occurs in locations where the river channel narrows and flow area is reduced by either a natural constriction of the floodplain, a bridge, or when overbank flow is redirected back into the channel by roadway embankments for the approach sections to a bridge. As the flow area is reduced through a contracted section, the increased velocity and shear stress exerted on the bed increases the sediment transport capacity and more sediment is removed from the contracted section than is transported into the section from upstream. This difference between incoming sediment supply and the transport capacity results in a lowering of the bed elevation with passage of large floods.

Under existing conditions, the channel is confined in the approach section upstream of the bridge crossing. The channel geometry approaching the bridge crossing was reconstructed following the river expansion and avulsion during the 1964 flood (Figure 9). In the current channel configuration, the Q100 wetted width is approximately 200 feet across near RM 44.8 and then narrows to about 80 feet in the approach section beginning about 400 feet upstream of the bridge. This channel configuration likely shifts the location of the greatest contraction scour to a point upstream of, rather than at, the existing bridge. The flow area in the confined approach section is 762 square feet and is contracted approximately 30% as it passes through the upstream opening of the bridge. Hydraulic analysis of the existing structure using the HEC-RAS model predicts a live-bed scour condition and a contraction scour depth of 2.4 feet at the bridge.

Contraction scour associated with an alternative to widen the existing crossing and replace the existing structure with two, 200-foot bridges is highly dependent on design criteria to be developed in later stages of the project. Initially, the proposed bridge would be expected to reduce contraction scour through the crossing because the abutments will be set back and decrease the flow constriction at the crossing. The proposed 200-foot span length crossing the

existing channel is approximately the same effective width of the less confined channel segment upstream neat RM 44.8. An important consideration, however, is how the channel will respond to future lateral channel changes. The northern-most of the two bridges in the proposed design crosses an old channel feature that is an avulsion hazard risk identified in previous assessment. Should future channel changes result in a considerable proportion of the flow being conveyed by this avulsion pathway, there is potential concern for contraction scour given that the relatively high skew angle of the proposed bridge would result in an effective bridge opening that will be less than the 200-foot span. In this potential future scenario, there could be a substantial contraction of flow at the bridge opening that would result in a considerably greater scour depth relative to the existing conditions. Calculation of this contraction scour requires additional information and design criteria.

The design alternative to relocate the bridge crossing to the upstream location near RM 44.6 with a structure combining four, 200-foot bridges is expected to result in only minor contraction scour. The channel opening under the bridge is essentially the natural channel width and the only structural element constricting flow would be the piers. Given the proposed pier spacing of 200 feet, only one pier is expected to interact with the flow at any given time as the channel migrates laterally. Comparison of the bridge section with the approach section in HEC-RAS did not calculate any contraction scour for the proposed design.

LOCAL SCOUR

Local scour is generated in locations that flow impinges on the upstream side of a pier or abutment, causing a redirection of flow that results in scouring forces at the base of the pier or toe of the abutment. Under existing conditions, local scour at the current bridge crossing is defined by the hydraulic conditions at the bridge abutments. The projected length of the flow obstruction is 11 feet at the left abutment and 5 feet at the right abutment at Q100. Using data from the HEC-RAS model as input to the Froehlich equation yielded an estimated scour depth of 24.2 feet.

The proposed design alternative to widen the existing crossing with two, 200-foot bridges would set the abutments outside of the Q100 flow area. Assuming sufficient countermeasures are installed to prevent lateral channel migration outside of the bridge abutments, there should be no flow interaction with the abutments and no local scour.

The proposed design alternative to relocate the bridge crossing to an upstream location near RM 44.6 with a structure combining four, 200-foot bridges is similarly assumed that bridge abutments are to be located outside the Q100 flow area. The concept design at this upstream location includes a drilled pile foundation with two, six-foot diameter columns spaced 18 feet apart. Pier scour at the upstream crossing was calculated from an iteration of the HEC-RAS model to generate hydraulic inputs for the CSU pier scour equation. Based on inputs from the conceptual design sketch, pier scour is estimated as 12.3 feet in the design alternative.

LATERAL CHANNEL CHANGES

Anticipating lateral channel migration is a key consideration in evaluating the design alternatives. The dynamic history of the Upper Sandy River underscores the need to consider future channel adjustments in relation to proposed bridge crossings. In regards to scour, lateral channel changes can result in future changes in geometry that may affect hydraulics though the bridge opening. Scour associated with anabranching channel patterns is another factor given that flow junctions where individual channel threads come together can result in scour on the order of twice the flow depth. Given the range of estimated flow depths in the project reach, the estimated scour at such junctions is estimated at approximately 6 to 8 feet.

The existing bridge condition has very little resilience to lateral channel migration as demonstrated by complete loss of the previous bridge following channel migration during the 1964 flood. Widening the existing crossing with two, 200-foot bridges will likely increase the resilience but is still vulnerable to shifts in channel position. A key concern with that scenario was addressed above in the discussion of contraction scour whereby there is potential risk of the primary flow being redirected into the avulsion pathway west of the current road alignment (old channel from 1964 flood). Given the high skew angle of the proposed road alignment relative to flow direction, the proposed alternative to widen the crossing at the existing location leaves some concern for future erosion hazards at the bridge.

Of the three scenarios considered, the alternative to relocate the road and construct a span with four, 200-foot bridges provides the greatest resilience to future lateral migration. This design scenario enables the greatest opportunity for the channel to adjust in response to future changes in channel alignment and/or episodes of channel aggradation.

SUMMARY

A preliminary assessment of factors affecting bridge scour was developed from review of hydraulic model results and evaluation of conceptual design sketches for proposed bridge crossings. A summary of total scour for the three alternatives is presented in Table 7. A summary of input parameters and results from the preliminary scour calculations follow in Table 8 and Table 9. Note additional design criteria are needed to determine the upstream approach section of the alternative to widen the existing crossing. The existing crossing is most sensitive to local scour where flow impinges on the left abutment. Design alternatives propose to set back and widen the crossing. Provided adequate countermeasures are employed to prevent lateral migration towards the abutments, the design alternatives should not have the same issues with local scour. The primary element of local scour in the proposed design alternative at the upstream crossing is the pier scour when piers are subject to flow. The pier scour calculation for a cylindrical 6-foot diameter column yielded a scour depth of approximately 12 feet. Factoring in the estimate of long-term degradation, these estimates are intended to give a general description of scour at proposed bridge crossings and are to be refined as part of the design process as additional criteria are specified for the proposed crossing.

Table 7. Summary of estimated scour depth for bridge crossing alternatives.

	No Action (Existing Conditions)	Alternative With Two, 200-Foot Bridges at Existing Crossing Location	Alternative With Four, 200-Foot Bridges at New Crossing Location near RM 44.6
Long-Term Degradation	6 ft	6 ft	6 ft
Contraction Scour	2.5 ft	<5*	0.7 feet
Pier Scour	N/A	N/A	12.3
Abutment Scour	24.2 ft	0 ft	0 ft
Total Scour	32.7 ft	11*	19 ft

* Contraction scour calculation for this alternative requires additional design information regarding partitioning of flow and proposed channel modifications in the approach section.

Table 8. Summary of input parameters and results from scour calculations at the existing bridge crossing representing the no action alternative.

Contraction Scour

Input Data	Left	Channel	Right
Average Depth (ft):	0.6	9.05	1.14
Approach Velocity (ft/s):	0.93	11.3	1.52
Br Average Depth (ft):		7.81	1.11
BR Opening Flow (cfs):		8547.4	2.6
BR Top WD (ft):		69.36	0.96
Grain Size D50 (mm):	32	32	32
Approach Flow (cfs):	1	8540.36	8.65
Approach Top WD (ft):	1.79	83.55	5
K1 Coefficient:	0.59	0.64	0.59
Results			
Scour Depth Ys (ft):		2.39	0
Critical Velocity (ft/s):		7.62	5.39
Equation:		Live	Clear

Pier Scour

Input Data	Left	Right
Station at Toe (ft):	8622.75	8693.07
Toe Sta at appr (ft):	9964.73	10040.06
Abutment Length (ft):	10.97	5
Depth at Toe (ft):	7.92	4.41
K1 Shape Coef:	1.00	
Degree of Skew (degrees):	90	90
K2 Skew Coef:	1	1
Projected Length L' (ft):	10.97	5
Avg Depth Obstructed Ya (ft):	7.67	1.14
Flow Obstructed Qe (cfs):	939.32	8.65
Area Obstructed Ae (sq ft):	84.14	5.69
Results		
Scour Depth Ys (ft):	24.15	3.24
Qe/Ae = Ve:	11.16	1.52
Froude #:	0.71	0.25
Equation:	Froehlich	Froehlich

Table 9. Summary of input parameters and results from scour calculations at the proposed bridge crossing alternative with four, 200-foot spans near RM 44.6.

Contraction Scour

Input Data	Left	Channel	Right
Average Depth (ft):	0.47	3.44	2.2
Approach Velocity (ft/s):	0.99	6.88	5.38
Br Average Depth (ft):		4.58	
BR Opening Flow (cfs):		8550	
BR Top WD (ft):		190.49	
Grain Size D50 (mm):	32	32	32
Approach Flow (cfs):	21.81	7883.39	644.8
Approach Top WD (ft):	47.53	333.36	54.59
K1 Coefficient:	0.59	0.64	0.59
Results			
Scour Depth Ys (ft):		0.7	
Critical Velocity (ft/s):		6.48	
Equation:		Live	

Pier Scour

Input Data	
Pier Shape:	Circular cylinder
Pier Width (ft):	6
Grain Size D50 (mm):	32
Depth Upstream (ft):	8.85
Velocity Upstream (ft/s):	10.43
K1 Nose Shape:	1
Pier Angle:	0
Pier Length (ft):	60
K2 Angle Coef:	1
K3 Bed Cond Coef:	1.1
Grain Size D90 (mm):	256
K4 Armouring Coef:	1
Results	
Scour Depth Ys (ft):	12.3
Froude #:	0.62
Equation:	CSU equation

CONCLUSIONS

EXISTING BRIDGE LOCATION

At the existing bridge location, the river flows through a single stem channel that is deeply incised between two terraces. The north terrace is composed of fill materials brought in to repair the bridge following the 1964 storm. The south terrace is composed of fill underlain by native soils. The channel/terrace/bridge embankment topography forms a narrow flow constriction, or pinch point, through which the velocities of most high stage flows accelerate. Both the existing height and topographic pinch point cause an upstream backwater condition, that induces bed load in transport to deposit on the channel floor upstream of the crossing. The depositional zone is prone to channel widening caused by aggradation and by northward channel migration. The northward migration caused substantial damage to Lolo Pass Road from RM 43.75 to RM 44.2 in 1964, 1996 and 2011 storm events.

An avulsion channel is situated on the north side of the bridge between E Lolo Pass Road and Clear Creek. This avulsion channel poses a substantial risk to the existing bridge and road alignment. Prior to the 1964 storm the avulsion channel was cut off from the main stem by E Lolo Pass Road. This channel is known to have received main stem flow during the 1964 storm; it received overbank storm flow during the period where the E Lolo Pass Road and embankment were breached. Existing 2015 conditions are essentially the same today as they were in 1964. The avulsion channel could receive main stem flow from any number of sites along E Lolo Pass Road (from RM 43.75 to RM 44.4) that are susceptible to damage from channel migration.

The results of the geomorphic/hydraulic analyses indicate the safest bridge/road alignment is one that routes the road along the high ground situated between the avulsion channel and Clear Creek (see Figure 27). The design alternative to widen the existing crossing with two, 200-foot bridges would certainly yield an improvement of flood conveyance through the crossing compared to existing conditions. Improvements to the bridge, however, are not enough to maintain safe access along this alignment given the number of erosion hazards affecting the road for nearly a mile upstream. At present the channel impinges on the road corridor upstream of the crossing near RM 43.8 and RM 44.1. Additional avulsion hazards are present throughout the reach where rapid shifts in the channel alignment could result in road damage from a single storm event. Any alternative in consideration that retains a road alignment in the valley bottom between the Sandy River and Clear Creek must acknowledge the ongoing maintenance costs to address erosion and damages to the roadway as occurred in 1964 and 2011.

PROPOSED UPSTREAM BRIDGE LOCATION

The proposed bridge location near RM 44.6 is situated in a very dynamic section of the river that is subject to periodic episodes of accelerated channel migration and sudden avulsion. The proposed site includes the main stem channel and a potential avulsion channel located on the north alluvial terrace. In this river section, there are two directional trends of migration, downstream (west) and lateral (north). These results indicate that as the large bend situated

upstream of the proposed crossing approaches the crossing alignment it will engage the full width of the currently active channel. Results also indicate the avulsion channel will receive main stem flow during a scenario where the channel upstream of the alignment is substantially aggraded during 100 year storm event. Geomorphic and hydraulic analyses both indicate the bridge design should span the currently active main stem channel and the full width of the potential avulsion channel (Figures 29 and 30). Over time, the Sandy River is expected to migrate laterally and reoccupy the historic flowpath on the north of the valley. Therefore, an open flowpath to the historical channel feature should be included in the road design criteria.

Compared to the alternative at the existing crossing, the proposed bridge location near RM 44.6 minimizes the long term risk to flood and erosion hazards. The design in this segment provides a longer span and is more resilient to lateral channel migration.

Sincerely,

Natural Systems Design, Inc.

Mary Ann Reinhart
Senior Geomorphologist

Tim Abbe
Principal Geomorphologist

Attachments:

REFERENCES

Bridge, J.S. 1993. The interaction between channel geometry, water flow, sediment transport and deposition in braided rivers. In: Best, J.L. and Bristow, C.S. (eds), Braided rivers. Special Publication of the Geological Society of London 75, 13-71.

Cameron, K.A. and P. Pringle. 1986. Post-glacial lahars of the Sandy River Basin, Mount Hood, Oregon. Northwest Science 60(4), 225-237.

Cooper, R.M., 2005. Estimation of peak discharges for rural, unregulated streams in Western Oregon, U.S. Geological Survey Scientific Investigations Report 2005–5116.

David Evans and Associates Inc., 2014. Reconnaissance Report for the Lolo Pass Road Access Alternatives Project, Prepared for the Western Federal Lands Highway Division.

DOGMAI (Oregon Department of Geology and Mineral Industries). 2011. LiDAR 0.04-meter RMSE Accuracy. Oregon LiDAR Consortium.

Eaton, B.C., R.G. Millar, and S. Davidson. 2010. Channel patterns: braided, anabranching and single thread. Geomorphology 120, 353-364.

Einstein, H.A., Barbarossa, N.L., 1952. River channel roughness. Transactions of the American Society of civil Engineers, 117(1), 1121-1132.

Elsner, M.M., Cuo, L., Voisin, N., Deems, J.S., Hamlet, A.F., Vano, J.A., Mickelson, K.E., Lee, S.-Y., Lettenmaier, D.P., 2010. Implications of 21st century climate change for the hydrology of Washington State. Climatic Change, 102(1-2), 225-260.

English, J.T., D.E. Coe and R.D. Chappell. 2011. Channel migration hazard maps for the Sandy River, Multnomah and Clackamas Counties, Oregon. Oregon Department of Geology and Mineral Industries Open-File Report 0-11-13.

Hamlet, A.F., Elsner, M.M., Mauger, G.S., Lee, S.-Y., Tohver, I., Norheim, R.A., 2013. An overview of the Columbia Basin Climate Change Scenarios Project: Approach, methods, and summary of key results. Atmosphere-ocean, 51(4), 392-415.

Hamlet, A.F., Lettenmaier, D.P., 2007. Effects of 20th century warming and climate variability on flood risk in the western US. Water Resources Research, 43(6).

Hydrologic Engineering Center. 2011. HEC-RAS River Analysis System. Version 4.1. U.S. Army Corps of Engineers. Davis, CA.

Jefferson, A. J. 2011. Seasonal versus transient snow and the elevation dependence of climate sensitivity in maritime mountainous regions.Geophysical Research Letters, 38(16). DOI: 10.1029/2011GLO48346

Manga, M., Kirchner, J.W., 2000. Stress partitioning in streams by large woody debris. Water Resources Research, 36(8), 2373-2379.

Mass, C., Skalenakis, A., Warner, M., 2011. Extreme precipitation over the West Coast of North America: Is there a trend? Journal of Hydrometeorology, 12(2), 310-318.

Natural Systems Design, 2015. Upper Sandy River Flood Erosion Hazard Mitigation Evaluation

Pierson, T.C., P.T. Pringle, and K.A. Cameron. 2011. Magnitude and timing of downstream channel aggradation and degradation in response to a dome-building eruption at Mount Hood, Oregon. Geological Society of America Bulletin 123, 3-20.

Scott, W.E., T.C. Pierson, S.P. Schilling, J.E. Costa, C.A. Gardner, J.W. Vallance and J.J. Major. 1997. Volcanic hazards in the Mount Hood Region, Oregon. U.S. Geological Survey Open-File Report 97-89. 16 p.

Sherrod, D.R. and W.E. Scott. 1995. Preliminary geologic map of the Mount Hood 30- by 60-minute quadrangle, Northern Cascade Range, Oregon. U.S. Geological Survey Open-File Report 95-219.

STARR (Strategic Alliance for Risk Reduction) 2012. Hydrology Report – Sandy River PMR. December. http://www.starr-team.com/STARR/Pages/default.aspx

STARR (Strategic Alliance for Risk Reduction) 2013. Hydraulics Report; Sandy River PMR – Oregon. http://www.starr-team.com/STARR/Pages/default.aspx

Tohver, I.M., Hamlet, A.F., Lee, S.Y., 2014. Impacts of 21st-Century Climate Change on Hydrologic Extremes in the Pacific Northwest Region of North America. JAWRA Journal of the American Water Resources Association, 50(6), 1461-1476.

U.S. Army Corps of Engineers. 1966. Postflood Report December 1964, January 1965 Flood, Portland District, Portland, OR. 107 p.

U.S. Geological Survey. 1914. Plan and profile of Sandy and Zigzag Rivers, Camp and Still Creeks, Oregon. Water Supply Paper 348. Washington D.C.

Warner, M.D., Mass, C.F., Salathé Jr, E.P., 2015. Changes in winter atmospheric rivers along the North American west coast in CMIP5 climate models. Journal of Hydrometeorology, 16(1), 118-128.

Wilcock, P.R., Pitlick, J., Cui, Y., 2009. Sediment transport primer: estimating bed-material transport in gravel-bed rivers.